MONITORING OF SIMULATED EROSIVE TOOTH WEAR BY CROSS-POLARIZATION OPTICAL COHERENCE TOMOGRAPHY

Maryam Abdulkareem Alghilan

Submitted to the faculty of the University Graduate School
in partial fulfillment of the requirements
for the degree
Doctor of Philosophy
in the School of Dentistry,
Indiana University

June 2019

Accepted by the Graduate Faculty of Indiana University, in partial fulfillment of the requirements for the degree of Doctor of Philosophy.

Doctoral Committee

_____
Anderson T. Hara, DDS, MSD, PhD, Chair

_____
Frank Lippert, MSc, PhD

April 30, 2019

_____
Jeffrey A. Platt, DDS, MS

_____
Carlos González-Cabezas, DDS, MSD, PhD

_____
Daniel Fried, BS, MSc, PhD

DEDICATION

To my wonderful parents Abdulkareem and Majidah and to my Sisters and Brothers. I love you and thank you for your endless love, support, and prayers.

ACKNOWLEDGEMENT

First and foremost, all praise and thanks to Allah for all the blessings in my life.

Then, I would like to acknowledge King Saud bin Abdulaziz University for Health Sciences and Indiana University for giving me the opportunity to pursue a PhD in Dental Sciences degree.

I would like to express my sincere thanks to my mentor Dr. Anderson T. Hara, who has been a constant source of knowledge and inspiration. This work would not be possible without his guidance. I am honored to have been able to work with him.

I would also like to extend my thanks to Dr. Frank Lippert, Dr. Jeffrey A. Platt, Dr. Carlos González-Cabezas, and Dr. Daniel Fried for their support and for providing valuable suggestions and advice on my dissertation. I am fortunate and honored to have such outstanding professors on my research committee. I am also thankful to Dr. Richard Gregory for his continuous support and guidance throughout my years in the PhD program.

Additionally, I am thankful to the family of the Oral Health Research Institute, including Sharon Gwinn, Adam Kelly, Nyi-Nyi Tin, Yuan Chen, Amnah Algarni, and Cecilia Turssi for their help and advice in the labs. Special thanks to all my friends in the PhD program who endlessly supported me during my PhD journey, particularly Sarah Al-Angari, Amnah Algarni, Afnan Alzain, Hadeel Ayoub, Alaa Sabra and Dawn Wagenknecht. Also, thanks to the awesome, supportive people I met during my PhD years.

My deepest gratitude and appreciation go to my parents and my siblings for their love, support, and encouragement.

Maryam Abdulkareem Alghilan

MONITORING OF SIMULATED EROSIVE TOOTH WEAR BY CROSS-POLARIZATION OPTICAL COHERENCE TOMOGRAPHY

Erosive tooth wear (ETW) is an emerging dental condition manifested clinically as tooth surface loss, eventually impairing the teeth's structural integrity, function, and esthetics. Both research and practice are in need of a quantitative, non-destructive method to monitor ETW. Cross-polarization optical coherence tomography (CP-OCT), an advanced imaging tool, shows great potential to fulfill this need, but its feasibility and shortcomings remain unclear. In this dissertation, I explored the capability of CP-OCT to monitor ETW in three in vitro studies, one per chapter. Chapter 2 investigated the effects of enamel surface roughness and dental erosion severity on CP-OCT dental surface loss measurements. Chapter 3 tested the effects of enamel surface roughness and dental erosion on CP-OCT enamel thickness measurements at different simulated wear levels. Chapter 4 explored the ability of CP-OCT to quantify the thickness of natural and worn-out enamel surfaces and to estimate longitudinally the wear depths resulting from simulated wear. I concluded: (1) enamel surface roughness did not affect CP-OCT measurements of enamel surface loss, however, the estimated error limited the appropriate assessment of the initial stages of dental erosion surface loss using CP-OCT; (2) enamel surface roughness and dental erosion did not affect CP-OCT enamel thickness measurements, and the CP-OCT differentiated the simulated enamel wear levels; and (3) CP-OCT quantified thickness of natural enamel before, during, and after the tooth wear simulation and allowed wear depth estimation following the simulated wear.

Anderson T. Hara, DDS, MSD, PhD, Chair

TABLE OF CONTENTS

LIST OF TABLES

LIST OF FIGURES

CHAPTER 1: GENERAL INTRODUCTION

Tooth enamel is the hardest substance in the human body, existing as a layer covering the coronal dentin and composed of a unique acellular, highly mineralized complex structure (Anderson and Creanor, 2016). This unique structure enables it to tolerate masticatory forces and to protect the underlying tooth tissues from the challenging environment in the oral cavity (Lu et al., 2012). Thus, maintaining the thickness of the enamel layer is of great importance for preserving the longevity, esthetics, function and structural integrity of the tooth, especially when considering the inability of the tooth to form new enamel (Nanci, 2013; Pandya et al., 2019). Yet the enamel surface is susceptible to non-carious chemical and mechanical attacks at physiological or pathological levels, causing an irreversible loss of enamel known as 'tooth wear'.

Tooth wear is a widespread dental condition in children, adolescents, and adults (Spijker et al. 2009; Kreulen et al., 2010). The mechanism by which tooth wear develops is complex and depends on the presence and possible interaction of the known main underlying mechanisms: dental abrasion, attrition, and erosion (Shellis and Addy, 2014). Dental abrasion occurs when the tooth surface is removed by an exogenous object or substance, such as toothbrushing using highly abrasive toothpastes (Ganss, 2014). Dental attrition is caused by abrasion from an opposing tooth or teeth as observed in bruxism (Ganss, 2014). Dental erosion is tooth surface loss caused by exposure to extrinsic (e.g. dietary) or intrinsic (e.g. gastric) acids of nonbacterial origin (Imfeld, 1996). These mechanisms often operate simultaneously and/or synergistically with one another to cause tooth wear (Ganss, 2014; Shellis and Addy, 2014). A combination of dental

erosion with abrasion or attrition, termed as erosive tooth wear (ETW), is the primary wear process observed clinically (Shellis and Addy, 2014).

ETW affects 46% of teenagers and 80% of adults in the United States as reported by the National Health and Nutrition Examination Survey (McGuire et al., 2009; Okunseri et al., 2014). In Saudi Arabia, 26-61% of examined children (Al-Majed et al. 2002; Al-Malik et al., 2002; Al-Dlaigan et al., 2017) and 28% of the examined adults (Johansson et al., 1996) had signs of ETW. Globally, the estimated mean prevalence ranges between 30-50% in deciduous teeth and between 20-45% in permanent teeth (Schlueter and Luka, 2018). All of these figures indicate that ETW is a prevalent oral health problem and requires attention in research and clinical practice.

The rate of enamel loss by tooth wear varies considerably among individuals and depends on the nature of the underlying mechanism (Kaidonis 1998), the degree of enamel resistance to wear (Lambrechts et al., 1989), and host protective factors that modulate the tooth wear process. Therefore, tooth wear should be monitored at the individual level to prevent further loss of the enamel and to control the wear process as early as possible. Additionally, clinical monitoring of tooth wear lesions will allow the testing of preventive interventions efficacy within the dynamic, complex conditions of the oral cavity at individual and population levels.

The available methods for clinical monitoring of ETW include analysis of tooth replicas directly and indirectly (Ganss et al., 2001; Bartlett, 2003), silicon putty impressions (Shaw and Smith, 1999), photographs (Wetselaar et al., 2016), and direct visual assessment with clinical scoring systems (Smith and Knight, 1984; Bartlett et al., 2008). While these methods can help in estimating the progression of tooth wear lesions,

accurate and objective quantification of lesion progression in a practical manner is still unfeasible owing to the available methods' limitations. Furthermore, some of these methods rely on comparing the affected tooth surface with a reference area, which can be subjected to loss or change over time, and affect the accuracy of the measurement.

Therefore, some objective clinically applicable methods have been proposed that use the dentinoenamel junction (DEJ) as a stable intraoral reference point for measurement (see the Appendix). Among the proposed approaches, the use of optical coherence tomography (OCT) offers remarkable advantages. OCT allows for obtaining the cross-sectional tomograms as well as 3D reconstructed enamel images non-invasively without X-ray ionizing radiation (Huang et al., 1991; Baumgartner et al., 2000; Fujimoto and Drexler, 2015).

OCT was invented for imaging of the retina and reported in 1991 (Huang et al., 1991). Since then, it has been significantly improved and its suitability investigated for a wide range of medical and dental applications. In dentistry, it has been tested in various fields including periodontics (Hsieh et al., 2011), endodontics (Shemesh et al., 2007), oral medicine (Jung et al., 2005), and cariology, where assessment of carious demineralization (Everett et al., 1999; Amaechi et al., 2001; Fried et al., 2002) has been reported. Polarization-sensitive OCT (PS-OCT) is an upgraded version of the conventional OCT, which includes co-polarization and cross-polarization components useful for imaging enamel optical changes. Changes in the optical properties of enamel (for instance, due to surface porosities or surface and subsurface demineralization/remineralization) can alter the incident OCT light scattering and penetration pattern. This alteration leads to a change in the polarization status of the backscattered light, which can be detected in the

output images of OCT (Baumgartner et al., 2000). Hence, areas of demineralization across enamel thickness can be identified and analyzed. This mechanism enables successful in vivo monitoring of caries progression (Louie et al., 2010).

The monitoring of enamel thickness with OCT was first proposed and tested by Wilder-Smith et al. (2009) to evaluate the enamel surface loss in patients with intrinsic dental erosion. The results of this study showed the ability of this method to quantify the enamel surface loss, but the authors suggested the need for further validation. The performance of this method has been tested on eroded (Chan et al., 2013) and sound enamel surfaces (Algarni et al., 2016) using PS-OCT. The enamel thickness measurement on eroded surfaces was found to be problematic and not always attainable (Chan et al., 2013; Aden et al., 2017) as it was in sound enamel (Algarni et al, 2016), because of the loss of DEJ reflection on the images.

As ETW lesions affect the enamel surface and thin subsurface area (Ganss et al., 2014), these lesions may react differently to incident polarized light. The increased surface roughness in eroded enamel might adversely affect the quality of the measurement as observed by Chan et al. (2013). However, to my knowledge, the effects of tooth surface changes on ETW measurements by cross-polarization OCT (CP-OCT) have not been evaluated yet. Furthermore, the studies tested severely eroded and surface-flat enamel, but it is not known how the method will perform on natural curved enamel surfaces. Therefore, my goal in this project was to evaluate the possible limitations and explore the full potential of CP-OCT for measuring and monitoring ETW. I explored the ability of an advanced commercially available CP-OCT device (Santec Inner Vision IVS-300-S-L-C; Santec Corp, Komaki, Japan) to quantify and monitor ETW by investigating

the effects of enamel surface micromorphology and demineralization severity on enamel thickness determination (from DEJ to enamel surface). My hypothesis was that CP-OCT can monitor ETW progression regardless of enamel surface and subsurface conditions. To test my hypothesis, I designed and conducted three laboratory experiments explained in detail in three chapters, each designed to address a specific aim as follows:

Specific aim 1 (Chapter 2): To determine the influence of surface roughness and dental erosion severity (determined by optical profilometry) on surface loss measurements (estimated from enamel thickness measurements) by CP-OCT. Human enamel specimens were prepared with three different surface roughness levels (very rough, rough, or polished), and each was subjected to a dental erosion challenge with a simulated dietary acid. Enamel thickness and surface loss measurements were taken from the specimen's center with OCT and optical profilometry, respectively at baseline and after 1, 2, 4, 6, 8, 16, and 24 h of dental erosion. The CP-OCT surface loss measurements were calculated and compared to surface loss values by optical profilometry.

Specific aim 2 (Chapter 3): To evaluate the effects of enamel surface roughness and dental erosion on enamel thickness measurements by CP-OCT, at different levels of simulated wear, as well as to compare the CP-OCT measurements with a standard method (micro-CT). Human enamel specimens with different surface micromorphologies (very rough, rough or polished) were prepared. Enamel thickness measurement with CP-OCT was conducted before and after dental erosion (10 min with citric acid). This cycle was repeated following wear simulation of approximately 300 µm and 500 µm. Lastly, enamel thickness was measured by micro-CT.

Specific aim 3 (Chapter 4): To investigate the ability of CP-OCT to quantify the thickness of natural- and worn-surface enamel and to estimate longitudinally the wear depths following simulated wear compared to micro-CT measurements. Natural unpolished human enamel slabs were subjected to five wear stages (1^{st}: to level the surfaces; 2^{nd}-5^{th}: < 100 μm) created by an automatic grinding/polishing machine. Enamel thickness was evaluated with CP-OCT and a standard method (micro-CT) at baseline and after every wear stage, then wear depths were measured for 2^{nd}, 3^{rd}, $4^{th,}$ and 5^{th} wear stages. The measurements among wear stages and between the methods were compared.

CHAPTER 2: IMPACT OF SURFACE MICROMORPHOLOGY AND DEMINERALIZATION SEVERITY ON ENAMEL LOSS MEASUREMENTS BY CROSS-POLARIZATION OPTICAL COHERENCE TOMOGRAPHY

2.1. Introduction

Dental erosion is an increasing oral health problem in modern societies (Jaeggi and Lussi, 2014). It is characterized by loss of dental hard tissues due to exposure to extrinsic (e.g. dietary) or intrinsic (e.g. gastric) acids (Imfeld, 1996; Huysmans et al., 2011). Appropriate clinical diagnosis and monitoring of dental erosion lesions would benefit from a method that yields objective and quantitative outcome measures. Of existing clinically available methods, optical coherence tomography (OCT) imaging technology holds promise. It is a non-destructive, sensitive (Huang et al., 1991) and safe (Nakagawa et al., 2013) clinical imaging tool. OCT technology can be used for various applications in dentistry (Jung et al., 2005; Shemesh et al., 2007; Louie et al., 2010; Hsieh et al., 2011). Since 1991, OCT was considered to have great potential for monitoring demineralization and remineralization in vivo (Amaechi et al., 2001; Fried et al., 2002; Jones and Fried, 2006). In the pioneering work of Wilder-Smith et al. (2009), an early OCT system was able to quantify enamel surface loss related to dental erosion in patients suffering from gastroesophageal reflux disease by measuring changes in enamel thickness.

Despite promising results, concerns have been raised with the use of OCT for this specific application, including the loss of DEJ resolution in images and unreliable measurements after extended periods of erosive challenge (Chan et al., 2013). It is well known that increases in surface scattering and demineralization can greatly attenuate the

penetration of the OCT signal interfering with the ability to resolve the underlying DEJ (Amaechi et al., 2001; Chong et al., 2007). During erosion, increased surface roughness and subsurface demineralization can both occur. It is unclear from prior studies to what degree increases in surface roughness contribute to the attenuation of the OCT signal. As the enamel surface micromorphology of erosive lesions may vary from rough with loss of luster in active lesions to smooth with some wear marks in inactive stages (Lussi et al., 2011), it is important to understand how changes on eroded enamel surfaces affect CP-OCT performance.

The objective of this study was to test whether enamel surface micromorphology and erosive severity (demineralization time) impact the ability of CP-OCT to quantify enamel surface loss. Optical profilometry was used as a gold standard method. A secondary objective was to test the repeatability of CP-OCT measurements.

2.2. Methods

2.2.1. Study design

In this in vitro study, I investigated the effects of two experimental factors on longitudinal measurement of enamel surface loss with CP-OCT: enamel surface roughness (very rough, rough, and polished) and severity of erosive demineralization challenge (1, 2, 4, 6, 8, 16, and 24 h). Human enamel specimens were prepared and distributed into three groups (n=10 each) according to their surface roughness. They were submitted to seven different levels of erosive challenge, and evaluated using CP-OCT and optical profilometry (gold-standard method) at baseline, and after each demineralization period. The primary outcome measure was enamel surface loss (in μm), calculated both by subtracting the enamel thickness (for CP-OCT) and enamel surface

profile (for profilometry) at each demineralization point from baseline. For the secondary objective of testing CP-OCT measurement repeatability, enamel thickness measurements (in μm) of original CP-OCT scans were compared with the measurements of the repeated scans from baseline, and after 4 and 24 h of demineralization. The experimental procedures including sample preparation and demineralization, profilometry and CP-OCT scanning and scan analysis were performed by one trained analyst (MAA).

2.2.2. Specimen preparation

Enamel slabs (4×4×2 mm) were prepared from coronal smooth surfaces of intact human molars using a low speed saw (IsoMet, Buehler, Lake Bluff, IL), flattened on the pulpal side and randomized into the surface morphology groups (very rough, rough and polished). Specimens were mounted on polishing disks with the enamel surface facing upward and stabilized with sticky wax. Next, the enamel surface was ground or polished with an automated grinding and polishing machine (Rotoforce-4, Struers Inc.) according to the roughness level for each group. The Specimens in the "very rough" group were ground flat with 500-grit SiC grinding paper (MDFuga, Struers). The specimens in the "rough" group were sequentially ground flat with 500-, 1200-, 2400-grit SiC papers. The specimens in the "polished" group were sequentially ground with 500-, 1200-, 2400-, 4000-grit grinding papers and then polished with 1-μm diamond suspension (DP-Suspension P, Struers). Specimens were then rinsed with deionized (DI) water, sonicated for 3 min in detergent solution and rinsed again with DI water for 3 min. The specimens' enamel surfaces were visually inspected to ensure no dentin was exposed. Specimens with areas of exposed dentin were excluded. Surface roughness was measured using an optical profilometer (see "Surface roughness measurement" section below). Ten

specimens from each group were chosen and removed from the polishing disks. Then, they were individually mounted on acrylic blocks and stabilized with cyanoacrylate adhesive. The occlusal surface of the specimen, which has the thickest enamel layer, was identified and the mounting block was labeled on the same side. Specimens were stored in a closed container in moist conditions to prevent specimen dehydration.

2.2.3. Surface roughness measurement

Surface roughness was measured by optical profilometry using an S5/03 sensor (Proscan 2000, Scantron, Venture Way, Tauton, UK) in a central area (2×2 mm) of the specimen and expressed in Ra values. The step size was set at 0.01 mm and the number of steps at 200 in the (X) axis; and at 0.1 mm and 20, respectively, in the (Y) axis. The scans were analyzed using the dedicated software (Proscan Application software v. 2.0.17) by applying auto leveling and surface filter function, which was set at 1. Then, Ra values in (X) and (Y) axes were recorded and averaged.

2.2.4. CP-OCT scanning and measurement

A commercial dental CP-OCT device (Santec Inner Vision IVS-300-S-L-C; Santec Corp, Komaki, Japan) was used to acquire the 3D scans. It uses a swept laser light source to generate the scans at a center wavelength of 1310 nm. The a-scan rate was 30 kHz and the range of imaging depth (in air) was 5.63 mm. The system's axial and lateral resolution (in air) was ≤ 12 μm and 30 μm, respectively. The scanning probe had a lateral scanning area of 5×5 mm and its working distance was 1 mm.

The specimen to be scanned was individually removed from the storage container, gently blot-dried at the surface with absorbent paper (KimWipes, Kimberly-Clark Corp.). Then, it was positioned on an X-Y and Z translation stage and under the CP-OCT sensor

with the labeled surface oriented toward the probe handle, which was fixed in a positioning arm. A 3D scan (5×5×5.63 mm) was performed for each specimen. The refractive index was set at 1.6. From the 3D scan, the central b-scan in X direction was selected and saved for measurements (position of the b-scan on the specimen is indicated in Figure 2.1). The positioning and scanning were performed within 2 min to ensure that adequate moisture was maintained in all specimens during scanning.

After obtaining the b-scans, the enamel thickness measurement (from DEJ to surface of the specimen) was performed in a blinded manner and it was based on the methods described by Chan et al. (2013) and Algarni et al. (2016). Briefly, the b-scan was opened in Santec Inner Vision IVS-300 software (Santec Corp, Komaki, Japan) then the measurement position (b) was identified at the center of the enamel width with the aid of a screen ruler (JR Screen Ruler, Spadix Software; www.spadixbd.com) (Figure 2.2). The DEJ measurement landmark along (b) position was annotated to help in identifying its depth on the b-scan (Figure 2.2). Then, the a-scan at (b) position was viewed by dragging the a-scan cursor line to position (b) (Figure 2.2) and clicking on "peak detect" function. On a-scan, the depths of the highest light intensity peaks at the enamel surface and DEJ areas were identified and confirmed by the depths of the measurement landmarks on b-scan (Figure 2.3). The distance between the depths of the two peaks on a-scan was calculated by clicking on "add layer" function. The distance in mm was recorded then converted to μm to represent the enamel thickness measurement at position (b). CP-OCT scanning and enamel thickness measurements were performed at baseline and following each demineralization period. To calculate surface loss, enamel thickness

measurements at every demineralization time point were subtracted from the baseline measurements.

2.2.5. Optical profilometric scanning and enamel surface loss measurement

Following enamel thickness measurements using CP-OCT, the specimens were scanned with an optical profilometer with a S5/03 sensor (Proscan 2000, Scantron, Venture Way, Tauton, UK). A central line (0.01×4 mm) was scanned, which overlaps the area of CP-OCT b-scan Y direction (Figure 2.1). The length of the scan covered both the treated and reference areas. Figure 2.1 shows the profilometric scanning line (dotted with pink lines). The step size was set at 0.01 mm and the number of steps at 400 in the (X) axis; and at 1 and 3 mm, respectively, in the (Y) axis. Surface profile analysis was performed with the use of a dedicated software (Proscan Application software v. 2.0.17) by applying a three-point height tool with an auto leveling function. Profilometric scanning and surface profile measurements were performed at baseline and following each erosive challenge. Then, the surface loss was calculated by subtracting enamel profile measurements at each demineralization time point from the baseline enamel profile measurements.

2.2.6. Dental erosion simulation

After CP-OCT/Profilometric scanning and before every erosive challenge, UPVC tapes were placed on two sides of the specimens to protect the reference areas from demineralization, leaving a testing area of 2×4 mm exposed in the center of the specimen surface (Figure 2.1). After each erosive challenge, the tapes were removed to allow the areas to be rescanned with CP-OCT and optical profilometry.

After generating CP-OCT and profilometric scans and test surface delimitation, the specimens were exposed to the demineralizing solution (0.3% citric acid, natural pH 2.40-2.41), at room temperature and with no agitation. A volume of 30 mL of demineralization solution was used per specimen. After immersion for the designated time, specimens were removed from the solution and rinsed thoroughly with DI water for 10 s. Specimens were then stored in humid conditions, in a sealed container. Measurements were performed after 1, 2, 4, 6, 8, 16 and 24 h of acid exposure, respectively.

2.2.7. Repeatability of CP-OCT measurements

For intra-examiner repeatability evaluation, a second set of 3D scans was performed for specimens at baseline, after 4 and 24 h of demineralization challenges. Enamel thickness measurements were repeated on the second 3D scans at least seven days after analyzing the original scans. The repeated measurements were then compared with the measurements of the original scans to evaluate the intra-examiner repeatability.

2.2.8. Statistical analysis

The effects of enamel surface roughness and demineralization time on surface loss (CP-OCT and optical profilometry) were analyzed using ANOVA. The ANOVA included fixed effects for roughness, demineralization time, and their interaction. Pairwise comparisons using ANOVA with a repeated effect were conducted.

Intraclass correlation coefficients (ICCs) and Bland-Altman plots were used to evaluate the intra-examiner repeatability of the CP-OCT and the agreement between the CP-OCT and optical profilometry surface loss measurements. Statistical analysis was

performed with SAS 9.4 (SAS Institute Inc., Cary, N.C., USA). A 5% significance level was used for all tests.

Figure 2.1. Schematic illustration showing specimen dimensions, position of the label, test and reference areas, position of CP-OCT b-scan, CP-OCT measurement position (b), and position profilometric scan.

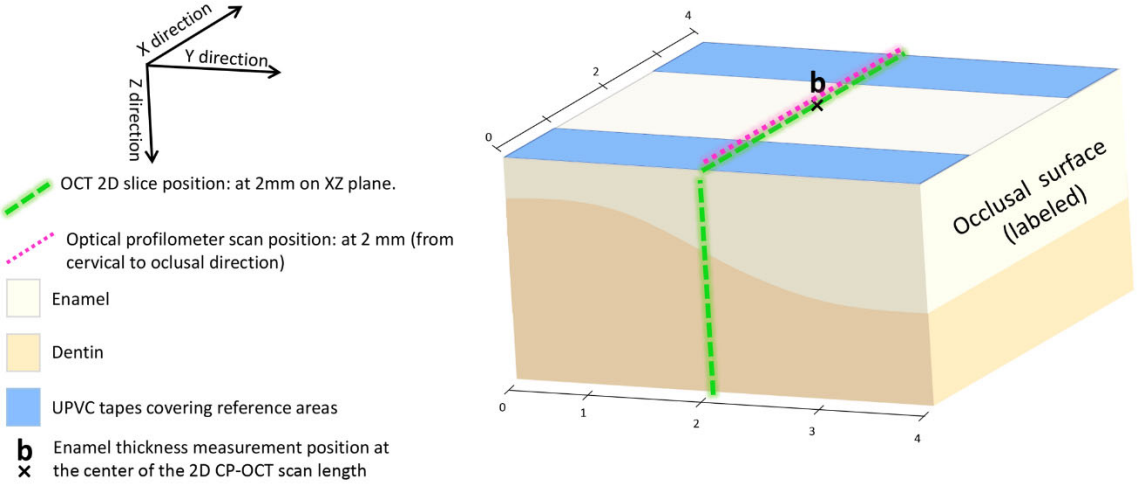

Figure 2.2. A screenshot showing a sample b-scan on the CP-OCT viewer and the JR screen ruler for locating the enamel measurement position (b) on the x- axis.

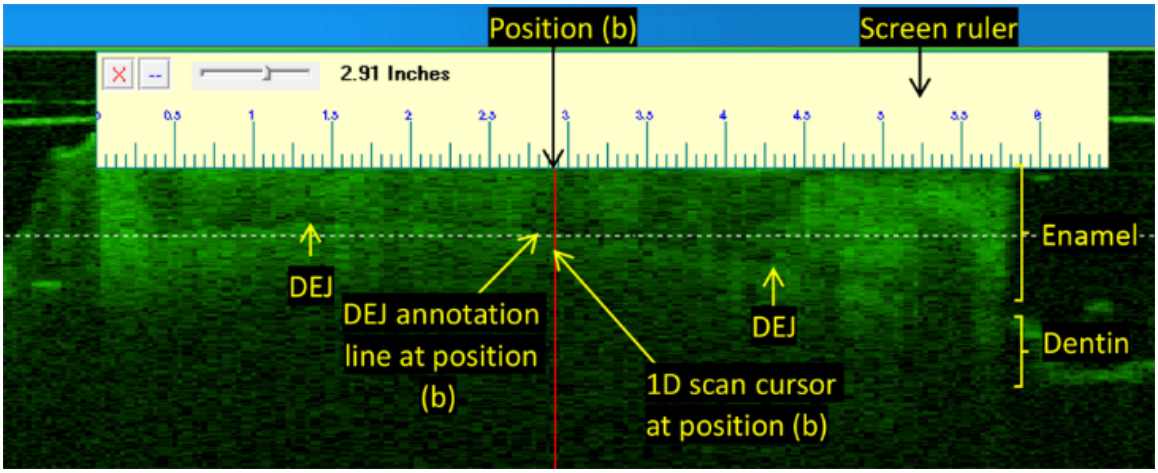

Figure 2.3. Enamel thickness determination using CP-OCT b-scan (left) and a-scan (right) along position (b) in the Z-plane. The position of the highest intensity peaks at the enamel surface and DEJ (indicated with labelled arrows) were identified. The distance between the two peaks was calculated by the "add layer" function, and distance in mm was recorded, which represents the enamel thickness measurement. The first high intensity peak above the enamel surface was ignored as it represents the probe's plastic cover placed for infection control purposes.

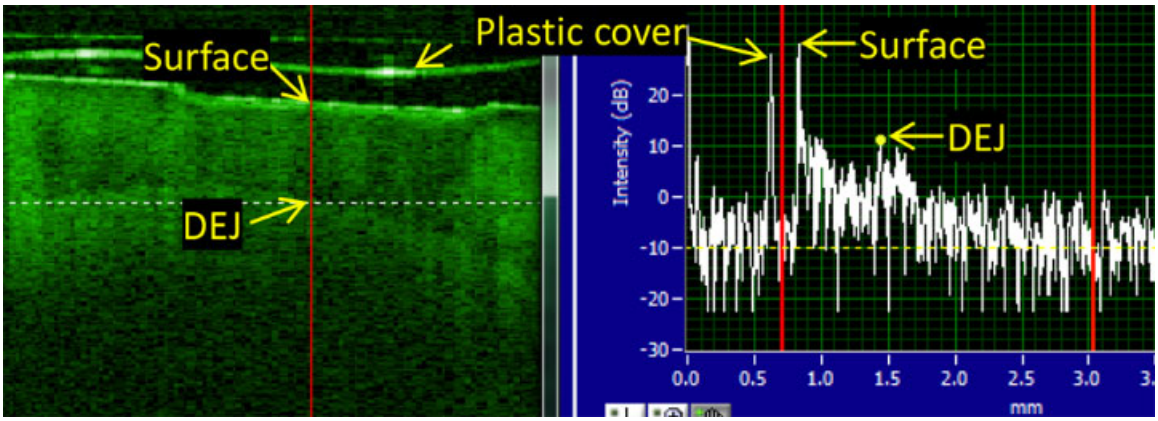

2.3. Results

2.3.1. Baseline enamel surface roughness characteristics

The mean ± standard deviation of enamel surface roughness at baseline, expressed in Ra parameter in µm, for very rough, rough and polished groups were 0.49 ± 0.07; 0.28 ± 0.04 and 0.10 ± 0.02, respectively.

2.3.2. Enamel surface loss with optical profilometry

There was no significant interaction effect (roughness × demineralization time) in enamel surface loss measurements ($p=0.75$). Among roughness levels, there were no significant differences in enamel surface loss measurements ($p=0.43$). However, among demineralization times, there were significant differences in measurements, with all of them differing from each other ($p<0.0001$; Table 2.1).

2.3.3. Enamel surface loss with CP-OCT

There was no significant interaction effect (roughness × demineralization time) in enamel surface loss measurements (p=0.49). Among roughness levels, there were no significant differences in measurements (p=0.27), and as with profilometry results, there were significant differences in measurements among demineralization times. Mean CP-OCT measurements after 1, 2, 4, and 8 h of demineralization were significantly lower than 16 and 24 h (P< 0.05); and 6 and 16 h were significantly lower than 24 h (P< 0.05). Table 2.2 shows the mean enamel surface loss measurements of CP-OCT for each roughness group and after each demineralization time, presented in µm.

2.3.4. Agreement between CP-OCT and Profilometry for enamel surface loss

Agreement between the two methods as evaluated by the intraclass correlation coefficient (ICC) and the mean difference is presented in Table 2.3. There was no significant difference between the methods' measurements means (p= 0.73). However, the ICC was poor (ICC=0.34). The Bland-Altman Plot (Figure 2.4) shows that the measurement error by CP-OCT was approximately ±150 µm compared to optical profilometry.

2.3.5. Intra-examiner repeatability for CP-OCT

Intra-examiner repeatability as evaluated by the difference between means, intraclass correlation coefficient and Bland-Altman plot can be found in Table 2.4 and Figure 2.5. There was no significant difference between the original and repeated measurements' means (p= 0.14). Additionally, the ICC was excellent (ICC=0.98). The Bland-Altman Plot (Figure 2.5) shows that the limits of agreement were at approximately ±150 µm.

Table 2.1. Mean ± standard deviation of enamel surface loss profilometry measurements (µm) for each roughness group and after each demineralization time.

	Demineralization time (h)								
	1	2	4	6	8	16	24	n	
Very rough	-5 ± 2	-9 ± 2	-20 ± 3	-29 ± 4	-39 ± 5	-70 ± 5	-105 ± 8	70	A
Rough*	-5 ± 2	-9 ± 2	-19 ± 7	-29 ± 7	-39 ± 7	-72 ± 9	-106 ± 8	35	A
Polished	-5 ± 1	-10 ± 1	-21 ± 2	-32 ± 2	-42 ± 4	-74 ± 6	-106 ± 6	70	A
n	25	25	25	25	25	25	25		
	a	b	c	d	e	f	g		

Similar uppercase letters in the last column represent no statistical difference among roughness groups means indicated by the ANOVA ($p > 0.05$)
Different lowercase letters in the last row represent statistical difference among demineralization times means indicated by the ANOVA ($p < 0.05$)
**Five enamel specimens from rough group were excluded from testing and analysis because their surface did not show signs of demineralization, possibly due to surface contamination with wax*

Table 2.2. Mean ± standard deviation of enamel surface loss CP-OCT measurements (µm) for each roughness group and after each demineralization time.

	Demineralization time (h)								
	1	2	4	6	8	16	24	n**	
Very rough	-16 ± 40	9 ± 83	-75 ± 69	-79 ± 128	-21 ± 67	-71 ± 17	-112 ± 27	54	A
Rough*	2 ± 7	-10 ± 13	-4 ± 37	-36 ± 36	-36 ± 20	-71 ± 12	-111 ± 28	25	A
Polished	14 ± 89	-1 ± 43	13 ± 69	0 ± 72	-17 ± 41	-75 ± 25	-113 ± 53	51	A
n**	17	19	19	21	20	16	18		
	a	a	a	ab	a	b	c		

Similar uppercase letters in the last column represent no statistical difference among roughness groups means indicated by the ANOVA ($p > 0.05$)
Different lowercase letters in the last row represent statistical difference among demineralization times means indicated by the ANOVA ($p < 0.05$)
**Five enamel specimens from rough group were excluded from testing and analysis because their surface did not show signs of demineralization, possibly due to surface contamination with wax*
*** Lower n values by CP-OCT compared to profilometry because DEJ was not clear in some CP-OCT scans*

Table 2.3. Agreement between Profilometry and CP-OCT enamel surface loss measurements according to the mean difference and intraclass correlation coefficient.

Profilometry vs. CP-OCT	Mean (SE) Profilometry (µm)	Mean (SE) CP-OCT (µm)	P-Value	SD within-sample (µm)	ICC
	-40 (4)	-39 (0.5)	0.73	44	0.34

SE-Standard Error; SD-Standard Deviation; and ICC-Intraclass Correlation Coefficient

Table 2.4. Intra-examiner repeatability analysis of CP-OCT original and repeated enamel thickness measurements (µm) for specimens at baseline, after 4 and 24 h of demineralization, according to the mean difference and intraclass correlation coefficient.

Original vs. repeated measurement	Mean (SE) original (µm)	Mean (SE) repeated (µm)	P-Value	SD within-sample (µm)	ICC
	958 (44)	943 (44)	0.14	53	0.98

SE-Standard Error; SD-Standard Deviation; and ICC-Intraclass Correlation Coefficient

Figure 2.4. Bland-Altman Plot for inter-method agreement.

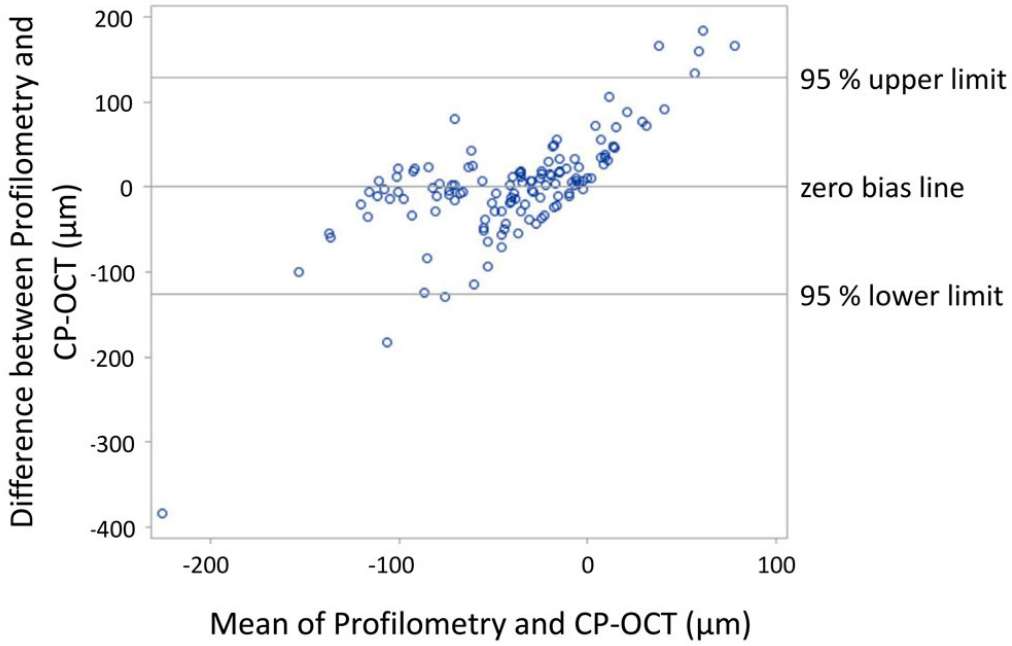

Figure 2.5. Bland-Altman Plot for showing the differences between pairs of CP-OCT enamel thickness measurements (µm) obtained from different scans and analyzed on different time points.

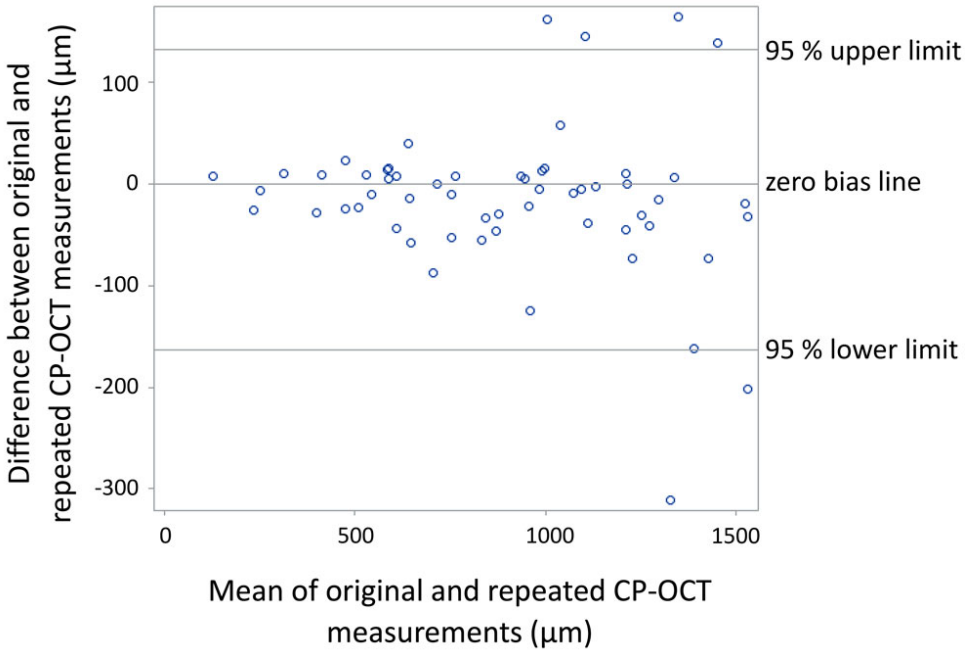

2.4. Discussion

In the present study, I tested whether enamel surface characteristics of roughness and demineralization by erosion simulation would affect CP-OCT measurements. Overall, my data showed that different levels of enamel surface roughness did not affect CP-OCT measurements.

Regarding the demineralization time effect, no significant differences were found among time points up to 8 h by CP-OCT. A possible explanation might be that the magnitude of early enamel surface loss remained below the resolution limit of the CP-OCT system. According to the manufacturer, the CP-OCT system's axial (depth or Z plane) resolution in air is ≤ 12 µm. Changes in the water content and variation in the

enamel composition with depth may cause small changes in the refractive index that can influence the path length (Chan et al., 2014).

Another possible explanation is the inherent measurement errors that were higher than the amount of enamel loss simulated at the early time points, as evidenced by the high standard deviation of the means, corroborating the findings of Chew et al. (2014). A possible source of error might be a slight shift in locating the measurement position in the 3D scan or b-scan or both, leading to measuring a different enamel position with a relatively longer or shorter enamel thickness. This limitation was also encountered when comparing and analyzing the before and after OCT images in a previous study (Tom et al., 2016), causing a larger error than the magnitude of the examined shallow lesions. Furthermore, potential errors could be related to difficulties in selecting the DEJ peak on a-scans for enamel thickness measurements, which are difficult to avoid due to the irregular nature of the DEJ (Chan et al., 2014). Additionally, the adoption of a plastic cover (infection control purposes) of the CP-OCT handheld probe may have caused uneven light refraction and attenuation patterns (Mandurah et al., 2013).

Despite the use of an advanced CP-OCT system under well-controlled laboratory conditions, I could not reliably detect surface loss of 7.2 μm, as reported clinically (Wilder-Smith et al., 2009). In that study and according to the authors, the process of the enamel thickness measurement and repositioning of the imaging probe using a stent was relatively unproblematic and they did not report any of the problems noted in the present or other studies (Huysmans et al., 2011; Chan et al., 2013).

On the other hand, after 16 and 24 h demineralization my results showed that the differences in surface loss by CP-OCT were significant and the results were more aligned

with profilometry mean enamel surface loss of 70 μm or more. It can be speculated that the loss of enamel thickness at the advanced demineralization timepoints reduced the light signal attenuation (Agrawal et al., 2013) and thus, improved the resolving capabilities of the OCT device, compared to the thicker enamel at early demineralization challenges. Chan et al. (2013) found that enamel thickness increased at 48 h of demineralization, when it was expected to decrease. My results differ from their observation, in fact the mean enamel thickness loss in my study at the maximum demineralization duration tested (24 h) showed a decreasing trend from previous timepoints and it is more consistent with profilometry data.

I was able to measure enamel thickness in most of the scans after every demineralization timepoint (1, 2, 4, 6, 8, 16 and 24 h; Table 2.2). However, I was unable to measure enamel thickness in some scans due to the loss of DEJ details. Similar observations were also reported by Chan et al. (2013) and Aden et al. (2017), who hypothesized that the difficulty in visualizing the DEJ in scans was in part due to specimens drying out during scanning (Chan et al., 2013). Demineralized dehydrated specimens caused increased light scattering because of a mismatch in refractive index, which in turn interfered with the light propagation deeper to the DEJ area (Chan et al., 2013). The loss of DEJ details in my study did not seem to be associated with the degree of demineralization. It is possible that this finding relates to the specimens' moisture condition during CP-OCT scanning (Shimamura et al., 2011). Chung et al. (2011) demonstrated the dramatic influence of internal hydration on the transparency of enamel at 1300-nm and have reported that it is extremely important that teeth are kept well hydrated for optical coherence tomography studies. In corroboration with earlier findings,

Hariri et al. (2013) and Nazari et al. (2013) have found a significant difference between OCT signals of enamel in wet and in dry conditions, with the difference being more pronounced in demineralized enamel, increasing with demineralization time. While there is still no consensus on the optimal hydration condition for specimens during OCT scanning (Shimamura et al., 2011; Austin et al., 2017), I controlled it during scanning to some extent by blotting the excess water and standardizing the time of the scanning procedure.

For CP-OCT agreement with optical profilometry for surface loss measurements, although the difference between the methods' measurements means was non-significant, the ICC value was low. Also, most of the differences presented in the Bland-Altman plot were larger than the magnitude of enamel surface loss measured by the gold-standard method. This indicates that the agreement of CP-OCT with optical profilometry was not satisfactory for measurement of enamel erosive surface losses created in this study. This could potentially be caused by the lower resolution of CP-OCT compared to profilometry (CP-OCT lateral and axial resolution= 30 μm and ≤ 12 μm, respectively in air; Profilometry S5/03 sensor resolution= 10 nm [0.01 μm]). Despite the low agreement with profilometry, the CP-OCT scanning and measurement approach used was repeatable. This may indicate that the measurement discrepancies were primarily due to changes of enamel optical properties associated with erosion simulation and the inherent disadvantages of the CP-OCT imaging and analysis approach used.

Both OCT and optical profilometry are non-contact, non-invasive technologies. They both use a light to acquire information from a specimen and are able to generate a two- or three-dimensional output (Schlueter et al., 2011). Profilometry also is the most

commonly applied quantitative method to measure enamel loss in in vitro and in situ studies, owing to its high sensitivity and accuracy (Schlueter et al., 2011); therefore, I employed it in this study as a gold standard method. Optical Profilometry was also used in the current study to characterize the enamel surface roughness changes using a commonly used roughness parameter in dental research, the arithmetic average (Ra) (Field et al., 2010). Measuring the surface roughness provides an information about the range of enamel surface roughness changes created in this study.

I utilized a 3D CP-OCT scanner to acquire b- and a- scans for analysis. With using the 3D OCT scanning system, the repositioning is potentially easier by having the outer borders of the specimen as landmarks for acquiring 3D repeated scans. Clinically, the gingival margin can be used as a position reference for repeated scans (Chan et al., 2016). Enamel thickness measurements were performed on raw b-scans and a-scans without rendering and analyzed using the associated software. This approach allows clear understanding of the device capabilities without analysis bias (Jansonius et al., 2016).

Dental erosion lesions are characterized by surface loss and a relatively small amount of subsurface demineralization that would most likely be few microns deep (Zentner and Duschner, 1996; Amaechi and Higham, 2001; Schlueter et al., 2009; Ganss et al., 2014). The extent of the subsurface portion of the lesion remains relatively constant as the dental erosion lesion progresses (Aden et al, 2017). Thus, enamel loss estimated from the changes in the enamel thickness measurements from the anatomical surface is more indicative outcome measure for monitoring changes during erosion progression.

In the proposed CP-OCT approach, the DEJ was considered as a reference because it has an advantage over the surface reference points that are subjectively

determined. An earlier study reported the difficulties with in vivo longitudinal measurement of maximum depth and horizontal width of NCCL lesions with using reference points on the enamel surface (Sugita et al., 2017). This was explained by the subjectivity in placing the reference points and by the changes in reference points positions due to abrasive loss at the tooth surface (Sugita et al., 2017).

There are some important limitations that need to be considered. Firstly, I performed the testing using surface-flat specimens, which does not reproduce the natural tooth curvature. It was necessary to flatten the surface to rule out any confounding factors related to variability in tooth curvature and to allow the surface to be analyzed accurately with optical profilometry. Secondly, the levels of surface roughness were not formed to simulate the roughness levels that occur in enamel erosion lesions inside the oral cavity. I arbitrarily created the degrees of enamel surface roughness to test the performance of the device on wide range of surface micromorphologies. Also, the continuous demineralization challenge induced in this study was planned to test the capability of the device to evaluate enamel surface loss and thus, to establish the device's usefulness for quantifying enamel thickness loss following dental erosion. Thirdly, the lower sample size in the 'rough' group. Five enamel specimens (50%) were excluded due to potential experimental error. It was observed that they had no measurable (by profilometry) demineralization, which was not as expected. I suspect that there was inadvertent enamel surface contamination with wax in those specimens, therefore justifying their exclusion from the study. In order not to interfere with the original randomization schedule and laboratory procedures initially planned, the samples were not replaced. Finally, I did not consider the presence of the acquired salivary pellicle. The pellicle can be visualized by

OCT (Baek et al., 2009) and possibly affect OCT signal intensity (Austin et al., 2017). It can also modulate the enamel surface roughness effect on the reflection intensity measurement because it fills the irregularities of the roughened enamel surface (Lussi et al., 2012). The magnitude of the pellicle effects on the outcomes of this study is unknown and should be further investigated. Within the above-mentioned limitations, this work provides valuable information regarding the capabilities and drawbacks of CP-OCT for enamel erosive surface loss measurement estimated from the remaining enamel thickness. The approach in this study seems to have little clinical applications for early stages of enamel erosive surface loss, owing to the unreliable surface loss measurements. On the other hand, the measurement approach showed to be practical and repeatable. Based on the significant demineralization effects on CP-OCT measurement, future studies will be aimed to elucidate the ability of CP-OCT to identify advanced erosive tooth wear levels and to clarify the effects of depth of demineralized enamel on the enamel thickness measurement by CP-OCT.

In conclusion, my results suggest that surface roughness changes do not affect CP-OCT measurements of enamel erosive surface loss. However, the estimated error observed for CP-OCT measurements limited the appropriate assessment of enamel erosive surface loss, in the magnitude simulated in this study.

CHAPTER 3: EFFECT OF ENAMEL ROUGHNESS, DENTAL EROSION AND WEAR SIMULATIONS ON CP-OCT ENAMEL THICKNESS MEASUREMENT

3.1. Introduction

Erosive tooth wear (ETW) represents the cumulative loss of dental hard tissues due to the exposure to extrinsic or intrinsic acids, combined with abrasive wear (Carvalho et al., 2015). ETW can adversely affect tooth form, function and esthetics, with potential signs of tooth sensitivity, ultimately leading to tooth destruction (El Wazani et al., 2012). The adoption of clinical measures for ETW prevention and control should be carried out as early as possible, associated with the monitoring of ETW lesion progression (Loomans et al., 2017). Clinical indexes have been used for this purpose, however, they are limited by their subjective nature (Amaechi, 2015). There is a need for a quantitative method to objectively assess and monitor ETW clinically.

I propose using enamel thickness changes to determine ETW progression, considering the dentinoenamel junction (DEJ) as a fixed measurement landmark. Potential clinical methods for this measurement include standard (periapical and bitewing) and specialized (computed tomography and cone beam computed tomography) radiographic methods, ultrasonography and optical coherence tomography. Advantages and disadvantages of these methods are summarized in the Appendix. Optical coherence tomography (OCT) technology stands out as a noninvasive, and highly sensitive imaging technology, which generates two- and three- dimensional cross-sectional images of the examined tissue in real time without using ionizing radiation (Huang et al., 1991; Baumgartner et al., 2000; Fujimoto and Drexler, 2015).

Sound human enamel manifests weak light scattering at 1300-nm (Fried et al., 1995; Darling et al., 2006), allowing penetration of light to a depth up to 3 mm (Colston et al., 1998), sufficient to enable the visualization of surface and subsurface structures of enamel including the DEJ. Demineralization can also be displayed and quantified successfully in OCT images, specifically by polarization-sensitive (PS) OCT (Baumgartner et al., 2000; Amaechi et al., 2001; Fried et al., 2002; Louie et al., 2010). OCT images of demineralized enamel show changes in light intensity and reflectivity as a result of increased light scattering and depolarization of the polarized incident light at demineralized zones (Everett et al., 1999; Darling et al., 2006). At the same time, the increased light scattering and depolarization greatly attenuate the light (Darling et al., 2006) reducing its penetration depth through enamel (Everett et al., 1999). This can potentially limit imaging capabilities of OCT for deep structures such as the DEJ in the presence of ETW lesions since they are characterized by tooth surface demineralization and increased surface roughness.

In the prior chapter, Chapter 2, I investigated the impact of different enamel roughness levels (very rough, rough and polished) and sequential demineralization (up to 24 h) on erosive enamel loss measurements by CP-OCT, estimated from enamel thickness measurements. I observed good alignment between CP-OCT and optical profilometry at surface loss larger than 70 µm. In this follow up study, I aimed to elucidate the effects of the decrease in enamel thickness by a laboratory simulated wear, surface roughness changes and a clinically relevant dental erosion challenge on CP-OCT measurements of enamel thickness. Also, I aimed to evaluate the agreement between CP-

OCT and micro-CT, a non-destructive gold-standard method, which allows accurate measurements of enamel thickness in vitro.

3.2. Methods

3.2.1. Study design

Human enamel specimens were prepared and distributed into three groups (n=8), and ground or polished according to the enamel roughness level (very rough, rough, or polished). Next, the specimens were evaluated using CP-OCT for enamel thickness measurement and with optical profilometry for surface loss and roughness measurements before and after an erosive demineralization challenge. After baseline (E0) measurements, the sequence of forming different roughness levels, demineralization and evaluation with CP-OCT and optical profilometry was repeated after two levels of simulated wear [approximately -300 µm (E1) and -500 µm (E2)] (Figure 3.1). Finally, the specimens were evaluated by a gold-standard method, micro-CT, for enamel thickness measurements, which were compared with CP-OCT measurements.

3.2.2. Specimen preparation

Unidentified intact extracted human molars, previously collected and stored in a tooth bank (IRB approval # NSO 911-07), were cut into blocks (4 mm × 4 mm × 2 mm) using a low speed saw (IsoMet, Buehler). They were flattened on the dentin side with an automated grinding and polishing machine (Rotoforce-4, Struers) and randomized into the three enamel micromorphology groups (very rough, rough or polished; n=8). Specimens of each group were mounted on a polishing block with the enamel surfaces facing upward and stabilized with cyanoacrylate adhesive and sticky wax. The specimens were labeled on the side of the polishing block.

At E0, the enamel surface was ground or ground and polished with the automated grinding and polishing machine. Enamel in the “very rough” group was flattened with 500-grit SiC grinding paper (MD-Fuga, Struers). Enamel in the “rough” group was flattened with 1200-grit SiC grinding paper. In the “polished” group, the enamel was flattened with 1200- grit SiC grinding paper, then polished with 2400-, 4000-grit grinding papers for 30 s each; and finally with 1-µm diamond suspension (DP-Suspension P, Struers) for 3 min. All specimens were then rinsed with deionized water, sonicated for 3 min in detergent solution and rinsed again with deionized water for 3 min. Enamel surfaces were visually inspected to ensure no dentin was exposed during sample preparation. Specimens were stored in a closed container with a relative humidity of approximately 100% to prevent specimen dehydration.

3.2.3. Wear levels

After baseline scanning before and after demineralization, the enamel thickness in each roughness group was subject to wear at two levels (E1 and E2; Figure 3.1) and enamel roughness levels were re-formed by the grinding and polishing procedures described in the previous section. The grinding time was guided by the target reduction depth at each wear level, which was -300 µm for E1 and -500 µm for E2. Specimen thickness was measured by a digital caliper (Fisherbrand Traceable Digital Caliper, Fisher Scientific), before and after the grinding procedure. Two measurements were recorded for each sample then averaged as the sample thickness measurement. The wear level was calculated by subtracting the sample thickness after wear from the thickness at E0, then the unit was converted into µm.

3.2.4. Enamel surface characterization with optical profilometry

A central area (2 mm × 1 mm) of the specimen (Figure 3.1) was scanned by optical profilometry (Proscan 2000, Scantron, Venture Way, Taunton, UK). The scan covered the treatment and reference areas on the enamel surface. The step size was set at 0.01 mm and the number of steps at 200 in the (X) axis; and at 0.2 mm and 5, respectively, in the (Y) axis. The scans were analyzed for surface loss and roughness measurements using the dedicated software (Proscan Application software v. 2.0.17).

Enamel roughness measurements were performed by analyzing the treatment area (0.4 mm × 1 mm). Auto-leveling and the level 1 surface filter were applied, then the average Ra value (in μm) along the (X) axis was recorded.

Enamel surface loss measurements were performed by analyzing the central line in the (Y) axis using a three-point height tool with an auto-leveling function.

Enamel surface loss and roughness measurements were performed before and after erosive challenge at each wear level. The change in enamel surface loss was calculated by subtracting surface loss measurements after demineralization from the measurements before demineralization for each wear level.

3.2.5. Enamel thickness determination with CP-OCT

A portable cross-polarization OCT (CP-OCT) device (Santec Inner Vision IVS-300-S-L-C; Santec Corp, Komaki, Japan), designed primarily for intraoral scanning, was used in this study. The device used a swept source laser light at a center wavelength of 1310 ± 30 nm to generate images in 3D (c-scan), 2D (b-scan) and 1D (a-scan). The a-scan rate was 30 kHz and the range of axial imaging (in air) was 5.6 mm and the depth of focus was 3 mm. The system's axial and lateral resolution (in air) was ≤ 12 μm and 30

μm, respectively. The maximum lateral scanning area of the probe was 5 mm × 5 mm and the probe's working distance was 1 mm.

The polishing block containing the specimens to be scanned was individually removed from the storage container, then all specimens were covered with absorbent paper (KimWipes, Kimberly-Clark Corp.) moistened with deionized water to prevent drying. The specimen to be scanned was gently dried with absorbent paper and positioned under the sensor of the CP-OCT probe with the labeled surface oriented toward the probe handle. The refractive index was set at 1.6 (Algarni et al., 2016) and a c-scan was performed and saved. After scanning, the specimen was immediately stored in moist conditions. From the c-scan, a b-scan at 2 mm of the specimen's length in the Y direction was selected and saved for measurements (b-scan location on the specimen is illustrated in Figure 3.1).

One analyst performed enamel thickness measurements in a blinded manner. Enamel thickness (from DEJ to surface of the specimen) was measured and analyzed at the central position on each b-scan by using Santec Inner Vision IVS-300 software (Santec Corp, Komaki, Japan). A screen ruler (JR Screen Ruler, Spadix Software; www.spadixbd.com) was used to locate the measurement position on the X-axis [position (b) at 2 mm of the specimen's width]. An a-scan was generated along position (b) on Z plane and used to identify the first change in the light intensity at the enamel surface and DEJ areas and then to measure the distance between the two identified peaks. The distance in mm was recorded, which represents the enamel thickness measurement along position (b) (Figure 3.2). CP-OCT scanning and measurement procedures were performed before and after the erosive challenge at each wear level. Figure 3.2 includes

representative CP-OCT b- and a- scans from “very rough” group taken at the different wear levels, before and after dental erosion.

3.2.6. Enamel thickness determination with micro-computed tomography (micro-CT)

A micro-CT scanner (Skyscan1172, Bruker microCT) was used to scan the specimens. Flat field correction was performed before each scanning session. The scanning settings were: filter - 0.5 mm aluminum, voltage - 59 kV, current - 167 μA, binning mode - medium, image pixel size - 5.88 μm, and frame averaging - 2. The specimens’ labeled side was marked and they were removed from the mounting blocks. An orientation notch was prepared on the dentin side of the mark using round carbide bur in a low-speed handpiece. Then, the specimens were stored individually in storage vials with a relative humidity of approximately 100%. The specimen to be scanned was removed from the storage vial, gently dried and wrapped with Parafilm to protect the specimen from dehydration. Each specimen was stabilized in a specimen holder with double-sided tape and individually scanned for 11 min.

The scans were reconstructed using the associated software (NRecon v1.7.3.1, Skyscan, Bruker microCT). The reconstruction settings applied were: smoothing - 2, post alignment - default, ring artifact correction - 20, beam hardening correction - 41, and the minimum and maximum attenuation coefficient values - 0 and 0.329744; respectively. The resolution of the reconstructed scans was 1500 × 1500 pixels.

The reconstructed scans were opened in the associated software (DataViewer v1.5.6.2, Skyscan, Bruker microCT) and oriented until the notch was facing the lower border of the X-Y plane view screen. With the help of the screen ruler (A ruler for windows v3.3.3), the central 2D slice in the X-Z plane was selected and saved for

measurement. Then, the saved 2D slices were converted into a bitmap with a scale bar using the analysis software (CT analyzer v1.17.7.2+, Skyscan, Bruker microCT). Specimen codes were generated, then all saved 2D scans were renamed to randomize them and to conceal their labels.

The coded micro-CT slices were analyzed in Image J (ImageJ 1.52a, NIH) for enamel thickness measurement. A screen ruler (A ruler for windows v3.3.3) was used to locate the measurement position [at the point dividing the length of the enamel into half (b)]. Then, the distance between the enamel surface and the DEJ was measured on the image using the line measurement tool. The distance in mm was converted into μm, representing the enamel thickness measurement along the measurement position.

3.2.7. Enamel demineralization by simulated dental erosion

The reference areas on the enamel surface were covered with unplasticized polyvinyl chloride (UPVC) tape before starting the demineralization challenge, leaving a treatment area of 1 mm × 4 mm exposed (Figure 3.1). Then, the specimens were immersed in the demineralizing solution (0.3% citric acid, natural pH, adjusted with 1 M KOH to pH 2.63) for 10 min at room temperature without agitation. A volume of 30 mL of demineralization solution was used per specimen. After dental erosion demineralization, specimens were removed from the solution and rinsed thoroughly with running deionized water for 15 s. The UPVC tapes were then removed to allow the areas to be rescanned with CP-OCT and optical profilometry.

3.2.8. Statistical analysis

Analysis of variance (ANOVA) was used to test for fixed effects of enamel roughness, demineralization and wear level on profilometry and CP-OCT measurements.

A repeated effect was included to account for the correlations within a specimen. Pairwise comparisons are made for all the outcomes among roughness groups, demineralization and wear levels. Intraclass correlation coefficient (ICC) and Bland-Altman plot were used to evaluate the agreement between the CP-OCT and micro-CT measurements. A 5% significance level was used for all the tests. Statistical analysis was performed with SAS 9.4 (SAS Institute Inc., Cary, N.C., USA).

Figure 3.1. Schematic illustration showing specimen dimensions, test and reference areas, location of CP-OCT b-scan, CP-OCT measurement position (b), and position profilometric scan at each wear level (E0 [Baseline], E1 [~-300 µm], and E2 [~-500 µm]).

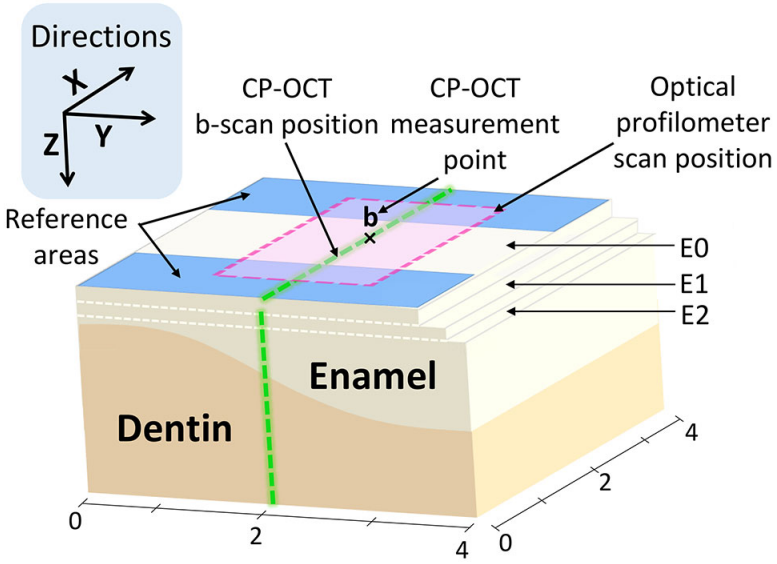

Figure 3.2. Representative CP-OCT b- and a- scans of a specimen, taken at the different wear levels (E0,1 and 2), before and after dental erosion.

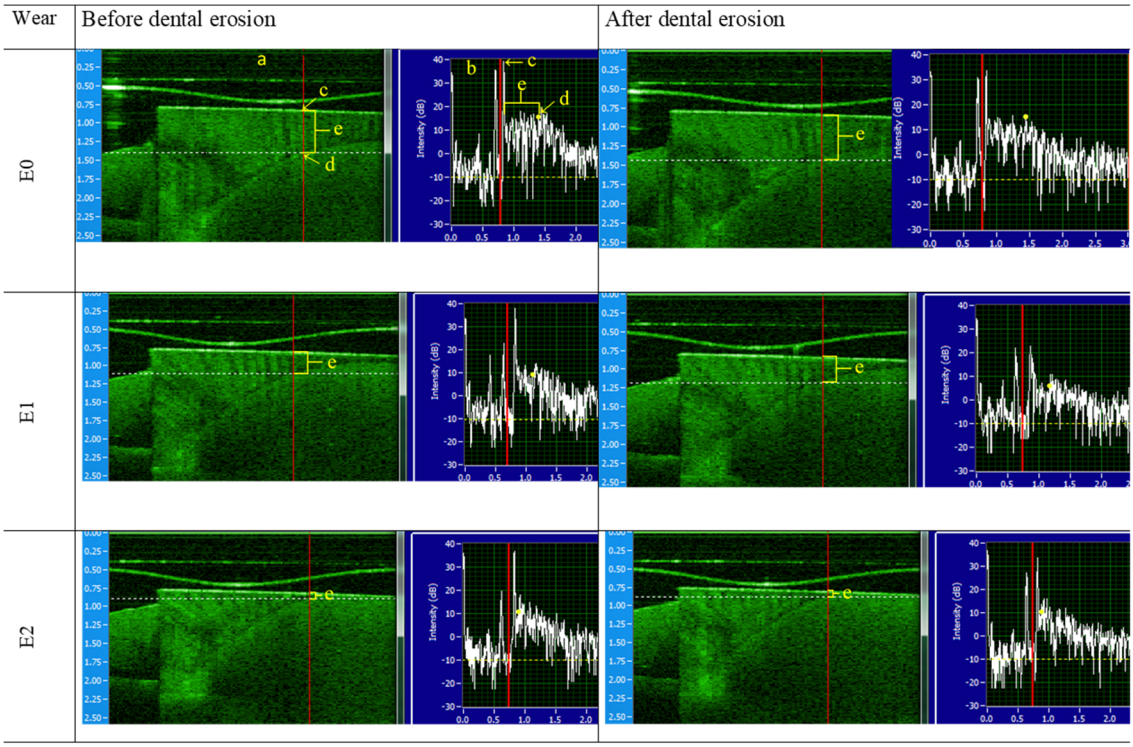

(a) b-scan; (b) a-scan; (c) enamel surface; (d) DEJ; (e) enamel thickness

3.3. Results

3.3.1. Wear levels

The mean ± standard deviation of E1, as measured by the digital caliper in µm, for the very rough, rough and polished groups were -256 ± 15; -320 ± 37 and -242 ± 37, respectively. The E2 for very rough, rough and polished group were -463 ± 19; -529 ±75 and -476 ± 56, respectively compared to E0.

3.3.2. Profilometry surface roughness analysis

Table 3.1 provides a summary of enamel surface roughness measurements before and after demineralization for very rough, rough and polished groups and at each wear level.

3.3.3. Enamel surface loss analysis

Mean and standard deviation surface loss measurements are highlighted in Table 3.2. For all roughness groups and wear levels, the range of the differences in mean enamel surface loss between before and after demineralization challenges were 0.98 μm to 1.86 μm.

3.3.4. Enamel thickness with CP-OCT

There were no significant two-way or three-way interactions in CP-OCT measurements among wear, enamel roughness, and demineralization ($p>0.34$). There were significant differences in measurements among wear levels ($p<0.0001$). CP-OCT enamel thickness measurements were significantly higher for E0 vs. E1 and E2 and for E1 vs. E2 (Figures 3.3-3.5). CP-OCT enamel thickness measurements were not significantly different among enamel roughness groups ($p=0.68$) or between before and after demineralization challenges ($p=0.40$). For all roughness groups and wear levels, the range of the differences in mean enamel thickness measurements by CP-OCT between before and after demineralization challenges was 5.49 μm to 102.26 μm. Mean enamel thickness measurements by CP-OCT are illustrated in Figures 3.3-3.5. In the rough group, enamel thickness measurement from one specimen in E1 before demineralization was not available because the DEJ was not visible in the CP-OCT scan. In the polished group, one specimen was excluded from analysis because the DEJ was not clear in scans at E1 and E2 before and after demineralization.

3.3.5. Agreement between CP-OCT and micro-CT

The inter-method agreement was high based on the difference between the mean measurements, ICC and Bland-Atman plot (Figure 3.6 and Table 3.3).

Table 3.1. Mean ± standard deviation of enamel roughness (Ra, µm) before and after dental erosion, at each wear level (E0-2).

Enamel	E0		E1		E2	
	Before demin	After demin	Before demin	After demin	Before demin	After demin
Very rough	0.51±0.04 a,A	0.45±0.04 b,A	0.50±0.08 a,A	0.42±0.05 b,A	0.60±0.06 a,A	0.47±0.04 b,A
Rough	0.34±0.04 a,B	0.38±0.03 a,B	0.36±0.04 a,B	0.38±0.04 a,A	0.43±0.05 a,B	0.38±0.05 b,B
Polished	0.18±0.06 a,C	0.40±0.07 b,AB	0.29±0.08 a,B	0.40±0.05 b,A	0.30±0.04 a,C	0.36±0.06 b,B

Different capital letters in the same column indicate significant differences between roughness groups, and different small letters in the same row within each wear level indicate significant differences before versus after demineralization.

Table 3.2. Mean ± standard deviation of enamel surface loss (µm) before and after demineralization for each roughness group at each wear level (profilometry measurements).

Enamel	E0		E1		E2	
	Before demin	After demin	Before demin	After demin	Before demin	After demin
Very rough	0.64±0.35 a,A	-0.67±0.49 b,A	0.51±0.11 a,AB	-1.30±0.38 b,A	0.76±0.72 a,A	-0.67±0.70 b,AB
Rough	1.25±0.56 a,B	-0.61±0.52 b,A	0.60±0.26 a,A	-0.74±0.08 b,B	0.85±0.45 a,A	-0.13±0.59 b,A
Polished	0.42±0.07 a,A	-0.98±028 b,A	0.18±0.09 a,B	-1.47±0.19 b,A	0.17±0.12 a,B	-1.06±0.30 b,B

Different capital letters in the same column indicate significant differences between roughness groups, and different small letters in the same row within each wear level indicate significant differences before versus after demineralization. Positive means indicate no surface loss or surface convexity; whereas negative means indicate surface loss.

Table 3.3. Agreement between CP-OCT and micro-CT expressed by the difference in the methods' measurements means and intraclass correlation coefficient (ICC).

CP-OCT vs. micro-CT	Mean (SE) CP-OCT (µm)	Mean (SE) micro-CT (µm)	P-Value	ICC
	654 (70)	683 (70)	0.20*	0.95

**No significant difference between methods' measurements means.*

Figure 3.3. Mean enamel thickness measurement by CP-OCT (in micrometers, μm) for the very rough group before and after erosive challenge at E0, E1, and E2 wear levels. The bars connected by a horizontal line are not significantly different ($p > 0.05$).

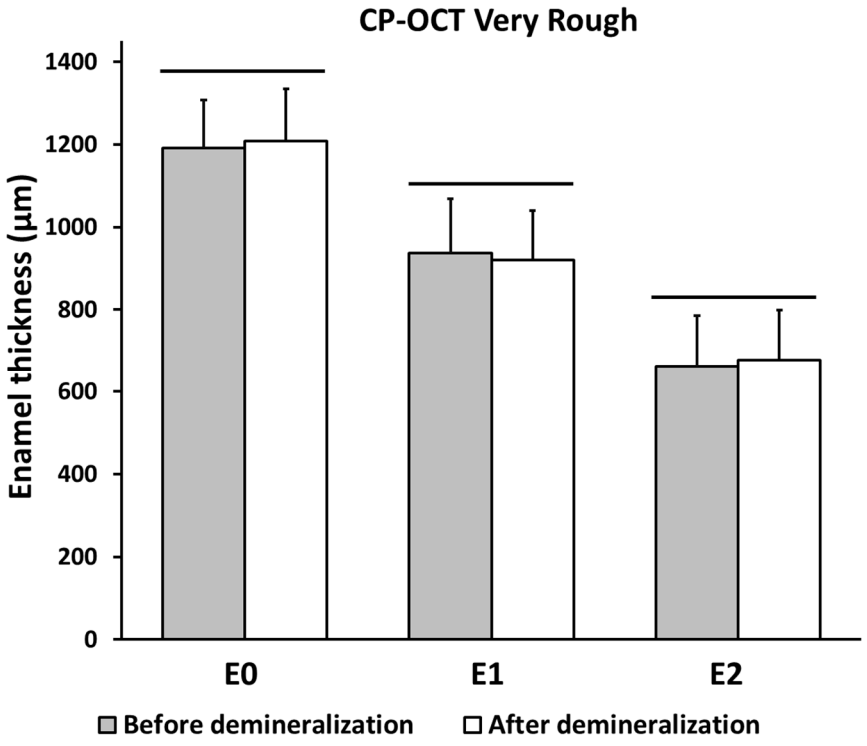

Figure 3.4. Mean enamel thickness measurement by CP-OCT (in micrometers, μm) for the rough group before and after erosive challenge at E0, E1, and E2 wear levels. The bars connected by a horizontal line are not significantly different ($p > 0.05$).

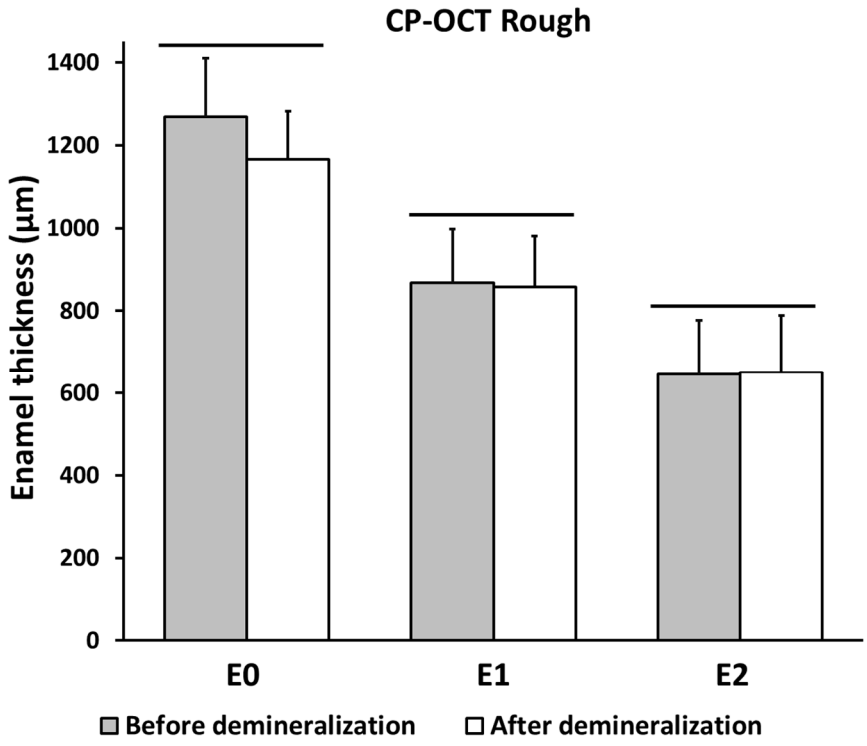

Figure 3.5. Mean enamel thickness measurement by CP-OCT (in micrometers, μm) for the polished group before and after erosive challenge at E0, E1, and E2 wear levels. The bars connected by a horizontal line are not significantly different ($p > 0.05$).

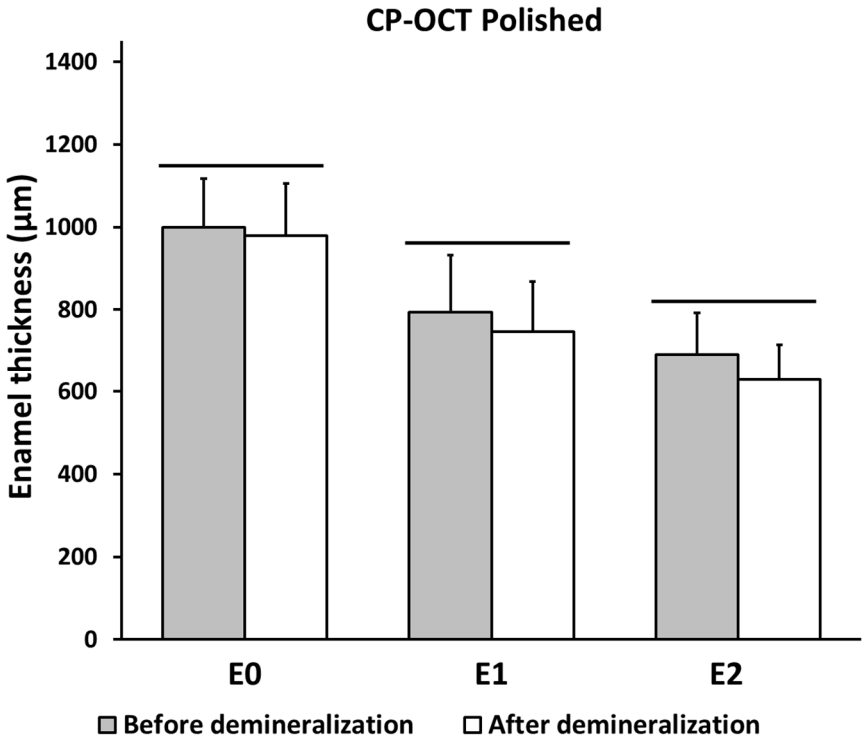

Figure 3.6. Bland-Altman plot, a graphical representation of the difference between the 23 measurements performed by CP-OCT and micro-CT. The range of agreement between the methods is approx. ±250 µm. Most of the measurements are within the range of agreement and scattered around the zero bias line within approx. ±100 µm.

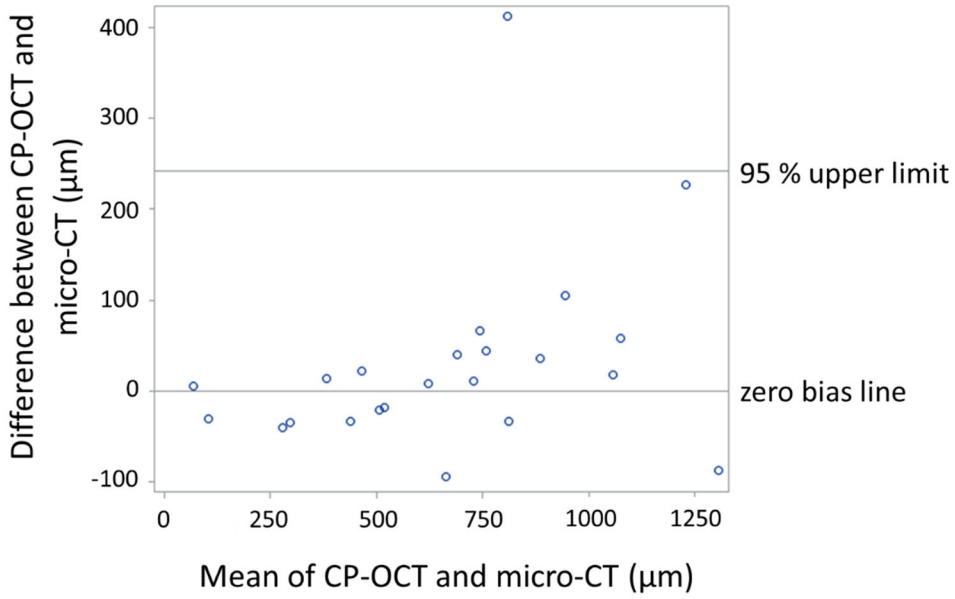

3.4. Discussion

Developing an objective method for the clinical assessment of ETW is one of the goals in this research field. OCT has shown to be a promising tool for this specific application (Wilder-Smith et al., 2009) despite some of its unforeseen drawbacks (Chan et al., 2013), therefore it requires further testing and validation. In this study, I focused on the effects of enamel surface micromorphology (roughness and demineralization) and wear levels on CP-OCT measurements.

The time of simulated dental erosion in my study was 10 min of acid exposure because the clinical exposure time of teeth to erosive acids is generally short before recovering of normal oral conditions as suggested by Jager et al. (Jager et al., 2012). I found no significant difference in enamel thickness measurements by CP-OCT between

before and after dental erosion, indicating that enamel surface demineralization by a short episode of erosion did not significantly affect CP-OCT measurements of enamel thickness, at all wear levels. It was also clear from Figure 3.2 that the tooth landmarks for enamel thickness measurement by CP-OCT were visualized in the specimens' scans in all enamel surface conditions before and after erosion.

In contrast, the effects of dental erosion on OCT measurements were noted in Chapter 2 and in Chan et al. (2013) because different dental erosion simulation models were used, involving prolonged acid exposure from 1 to 24 h (Chapter 2), and up to 48 h (Chan et al., 2013). Although clinically not relevant, these extended demineralization times aimed to simulate advanced erosion inducing enamel surface loss. Based on the ability of CP-OCT to resolve DEJ landmark in the scans of the current study and the previous studies, I suggest that the prolonged enamel exposure to erosive acid for more than 1 h may reduce the OCT optical path length and visibility of DEJ; therefore impacting the enamel thickness measurements.

Despite the non-significant demineralization effect with 10 min dental erosion challenge, the differences (not statistically significant) observed in enamel thickness measurements ranged from 5.49 μm to 102.26 μm. This is much higher than that observed with optical profilometry (from 0.98 μm to 1.86 μm). The higher difference observed by CP-OCT could be attributed to the difficulty in repeating measurements in the same position, as reported in Chapter 2. If practicality is not a concern, repeated measurement error can be minimized by using a positioning stent fabricated for each specimen at the baseline then used on the consecutive scanning sessions to orient the scanning probe to the same location. This approach was reliably used by Wilder-Smith et

al. (2009) for enamel thickness measurements in patients with advanced dental erosion and gastroesophageal reflux disease (GERD).

Despite the observed variation, CP-OCT measurements highly agreed (ICC=0.95) with those of micro-CT. These findings correspond well with the previous inter-method agreement between PS-OCT and micro-CT for measuring sound enamel thickness (ICC =0.95) (Algarni et al., 2016).

As for surface roughness effects, I found no significant differences in CP-OCT enamel thickness measurements among all enamel roughness groups. Further analysis also showed that each enamel roughness tested, with or without demineralization, did not impact enamel thickness measurements by CP-OCT as seen in figures 3.3-3.5. This result has further supported my previous observations in Chapter 2 related to the lack of influence of enamel surface roughness on enamel thickness measurements by CP-OCT.

The depth of remaining enamel thickness did not seem to affect the ability of enamel thickness measurement by CP-OCT and the quality of the measurements. This was depicted by the visibility of the measurement landmarks and the nearly similar standard deviation at each wear level (Figures 3.2-3.5).

Additionally, there was a significant decrease in enamel thickness measurement by CP-OCT from E0 to E1 and to E2, as expected. These differences among wear levels are meaningful because they indicate that CP-OCT allows identification of enamel loss of approximately 200 and 300 μm due to the wear process, in the presence or absence of demineralized roughened enamel surfaces.

It is interesting to note that in this study, CP-OCT enabled measuring very thin enamel near exposed dentin under all tested conditions. This is particularly helpful to

overcome the problem of unsatisfactory agreement in the distinction between enamel and dentin erosive tooth wear lesions with the use of erosive wear clinical scoring systems (Ganss et al., 2006; Mulic et al., 2010).

My earlier work, Chapter 2, highlighted several key strengths for the approach used in this study including assigning the DEJ depth as a fixed reference point for monitoring of changes in enamel thickness. In addition, a-scans were selected from the 3D scans followed by b-scans, for more precise localization of the measurement position.

The study is limited by the possible measurement errors related to the repeated selection of the measurement site as reported in the prior chapter, Chapter 2. A technical difficulty was keeping the protective plastic sleeve cover of the scanning probe away from the specimen during scanning while maintaining an appropriate working distance between the sample and the scanning probe. A probe adapter fabricated and described by Chan et al. (2016) would better secure the plastic cover during scanning, minimizing interference. One specimen was excluded from the analysis because the DEJ could not be traced in b-scans, either prior to or after the dental erosion challenge.

This study tested flat enamel surfaces and simulated only a few aspects of ETW. Some relevant factors such as saliva and salivary pellicle were not reproduced and therefore the findings should be interpreted with caution. Despite these limitations, the results were very encouraging and provide further support for the use for CP-OCT for monitoring of erosive tooth wear lesions. Future work should consider investigating natural enamel surfaces and more clinically relevant conditions.

In conclusion, the simulated changes in enamel thickness and surface micromorphology did not impact enamel thickness measurement by CP-OCT. CP-OCT

agreed well with micro-CT for enamel thickness measurements on eroded surfaces. CP-OCT was able to differentiate the wear levels simulated in this study.

CHAPTER 4: *IN VITRO* LONGITUDINAL EVALUATION OF HUMAN ENAMEL WEAR USING CROSS-POLARIZATION OPTICAL COHERENCE TOMOGRAPHY

4.1. Introduction

Tooth wear is the irreversible loss of dental hard tissue of either physiological or pathological nature. The rate of pathological enamel loss varies considerably among individuals and depends on the nature of the underlying related wear mechanisms, whether abrasion, erosion, attrition or abfraction, combined or not (Kaidonis et al., 1998), and the degree of enamel wear resistance (Lambrechts et al.,1989). Therefore, tooth wear should be clinically monitored and controlled, preferably using objective methods.

Among the available potential methods, optical coherence tomography (OCT) offers remarkable advantages, as it allows a quantitative analysis of enamel thickness to be performed at chairside. Additionally, OCT creates cross-sectional tomograms as well as 3D reconstructed enamel images non-invasively without X-ray ionizing radiation (Huang et al., 1991; Baumgartner et al., 2000; Fujimoto and Drexler, 2015). Those tomographic images enable dentin-enamel junction (DEJ) visualization, which can be used as a landmark, ruling out the need for intact enamel surface or artificially created reference areas or points for tooth wear measurement. This approach was first proposed and tested by Wilder-Smith et al. (2009) to evaluate enamel erosive tooth wear by endogenous acids, although further validation was deemed necessary. The performance of this method was also tested on eroded enamel surfaces in Chapter 2 and in Chan et al. (2013). However, these studies considered the simulation of severe dental erosion and use

of surface-flat enamel. Moreover, the capability of this approach to detect lower enamel wear rates has not been explored.

The objectives of this study were to a) evaluate the accuracy of enamel thickness measurements performed by CP-OCT for enamel with natural, unpolished surfaces compared to measurements by micro-CT, and b) to evaluate the capability of CP-OCT to quantify the progression of enamel wear from enamel thickness and wear depth measurements, compared to micro-CT measurements.

4.2. Methods

4.2.1. Study design

Human enamel specimens were submitted to five wear stages created by use of an automatic grinding and polishing machine and guided by digital micrometer specimen thickness measurements. Enamel thickness was evaluated by a trained analyst with CP-OCT and the gold-standard method, micro-CT, at baseline (natural tooth surface), and after every wear stage. The capability of CP-OCT to measure the thickness of natural-surface and worn-surface enamel and to differentiate the wear depths was assessed and compared to the gold-standard method.

4.2.2. Natural-surface enamel specimen preparation

Extracted intact human molars previously collected and stored in a tooth bank (IRB approval # NSO 911-07) were used to obtain the study's specimens. Ten enamel slabs (4 mm × 4 mm × 2 mm) were cut from smooth surfaces of the molars using a low speed saw (IsoMet, Buehler, Lake Bluff, IL). Then, they were mounted on an acrylic polishing block with the dentin side facing upward and stabilized with sticky wax. The specimens' dentin surface was flattened with #500 grit SiC paper (MDFuga, Struers) on

an automated grinding and polishing machine (Rotoforce-4, Struers Inc.) under running deionized (DI) water. An orientation notch for remounting and scanning was prepared on the center of the outer dentin edge using a round carbide bur in a low-speed handpiece. Specimens were then removed from the block, cleaned of wax and each stored individually in a closed labeled vial in humid conditions to prevent specimen dehydration.

4.2.3. Wear stages

The specimens' enamel surface was reduced in five stages: Wear 1 (to flatten the enamel surface); Wear 2, 3, 4 and 5 (target wear depth: 0.05±0.02 mm for each stage). At each wear stage, the specimens were re-mounted on an acrylic polishing block with the enamel surface facing upward and stabilized with sticky wax. On the automated grinding and polishing machine, the enamel surface was reduced with #1200 SiC paper then polished with #2400 and #4000 grit SiC papers and finally with 1-µm diamond suspension on a polishing cloth. The grinding time was guided by target wear depth; thus, specimens' thicknesses were measured with a digital micrometer indicator (Brown & Sharpe Digit-Dial Plus Indicator #599-1033) before, during and after the grinding procedure. Each sample thickness measurement with the digital micrometer was an average of two measurements. After grinding/polishing, the specimens were rinsed with DI water for 3 min, cleaned in an ultrasonic bath with a detergent solution for 3 min then rinsed with DI water for 3 min. Specimens were then removed from the mounting block, cleaned and stored as described in subsection 4.2.2.

4.2.4. Enamel thickness and wear depth evaluation with CP-OCT

A cross-polarization OCT (CP-OCT) dental imaging device (Santec Inner Vision IVS-300-S-L-C; Santec Corp, Komaki, Japan) was used in this study to obtain and analyze cross-sectional images of the enamel. The device uses a swept source laser light at a center wavelength of 1310±30 nm,with a scan rate of 30 kHz. The device's maximum lateral scanning area was 5 mm × 5 mm with axial and lateral resolutions (in air) of 12 μm and 30 μm, respectively. The range of axial imaging (in air) was > 5.6 mm and the depth of focus was 3 mm.

The specimen to be scanned was gently air dried for 10 s then positioned under the sensor of the CP-OCT probe with the notch oriented toward the probe handle. In the scanning and analysis software (Inner Vision IVS-300, Santec Corp, Komaki, Japan), a 3D scan (5 mm × 5 mm × 5.6 mm) was obtained for each specimen at refractive index = 1.6 (Algarni et al., 2016). After scanning, the specimen was kept in the storage vial.

For randomized and blinded analysis, specimen codes were generated and used to rename the 3D scans. From each 3D scan, the central b-scan in the Y direction was selected and saved to be evaluated for enamel thickness measurements. On the b-scan, three measurement positions were located at the half (b) and thirds (a and c) of the enamel width using a screen ruler (A ruler for windows v3.3.3) (Figure 4.1). Enamel thickness distance in mm (from DEJ to surface of the specimen) was measured at each of the three positions by measuring the distance between the depth of light intensity change at the enamel surface and the DEJ from each a-scan (Figure 4.1).

CP-OCT scans were obtained and analyzed for enamel thickness measurement before wear (natural-surface enamel) and after every wear stage. The wear depth

measurement by CP-OCT was estimated by subtracting the enamel thickness measurement after each wear stage from Wear 1 measurement.

4.2.5. Enamel thickness and wear depth evaluation with micro-CT

An X-ray micro-computed tomography (micro-CT) scanner (Skyscan1172, Bruker microCT) was used as a gold-standard method to obtain cross-sectional images of the enamel. The specimens were scanned at 59 kV and 167 μA with 0.5 mm aluminum filter using medium binning mode and an image pixel size set at 5.88 μm (Algarni et al., 2016).

The scans were reconstructed on the reconstruction software (NRecon v1.7.3.1, Skyscan, Bruker microCT) using smoothing at 2, post alignment at -5, ring artifact correction at 20, beam hardening correction at 41, and the minimum and maximum attenuation coefficient values at 0 and 0.329744, respectively.

The reconstructed scans were viewed on the associated software (DataViewer v1.5.6.2, Skyscan, Bruker microCT) to obtain the central X-Z image that corresponds to the CP-OCT b-scan position. To locate the central X-Z image, the reconstructed scan was viewed on the X-Y plane and oriented until the notch was facing the lower border of the viewer. Then, the screen ruler was used to locate half of the enamel width on the Y-axis. At the located point, the X-Z image was viewed and saved for enamel thickness measurement.

Then, the saved X-Z image (8.817 mm × 3.527 mm) for each specimen was converted into a bitmap with a scale bar using the analysis software (CT analyzer v1.17.7.2+, Skyscan, Bruker microCT). Specimen codes were generated and used to rename the images for blinded and randomized analysis.

The coded images were opened in Image J (ImageJ 1.52a, NIH) for enamel thickness measurement. On the image, three measurement positions were located at the half (b) and thirds (a and c) of the enamel width using the screen ruler (A ruler for windows v3.3.3) (Figure 4.2). Enamel thickness distance in mm was measured at each of the three positions by measuring the distance between the enamel surface and DEJ using the straight line tool (Figure 4.2).

Micro-CT images were obtained and analyzed for enamel thickness measurement before wear (natural-surface enamel) and after every wear stage. The wear depth measurement by micro-CT was estimated by subtracting the enamel thickness measurement after each wear stage from Wear 1 measurement.

4.2.6. Statistical analysis

Agreement between CP-OCT and micro-CT for thickness measurement of natural-surface enamel was evaluated using an intra-class correlation coefficient and the significance of the difference between the methods' means. Agreements between the methods for thickness measurement of worn enamel and wear depth estimation were evaluated using intra-class correlation coefficients, the significance of the difference between the methods' means, and Bland-Altman plots.

The effects of wear stages on enamel thickness and wear depth measurements by micro-CT and CP-OCT were tested using ANOVA followed by pairwise comparisons. The ANOVA included a random effect to account for correlations among the three enamel positions within each specimen, and a repeated effect to account for the correlations among the wear stages. A 5% significance level was used for all the tests. Statistical analysis was performed with SAS 9.4 (SAS Institute Inc., Cary, N.C., USA).

Figure 4.1. CP-OCT b-scan (left) and a-scan (right) analysis for enamel thickness measurements.

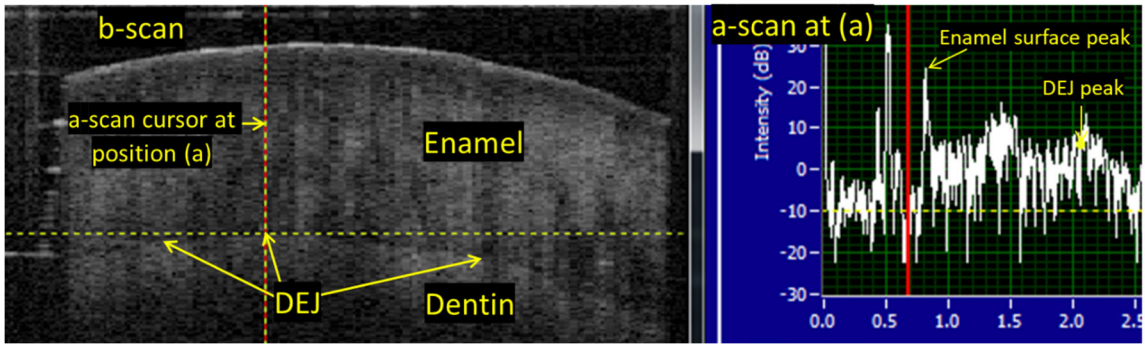

Figure 4.2. Micro-CT image analysis for enamel thickness measurements.

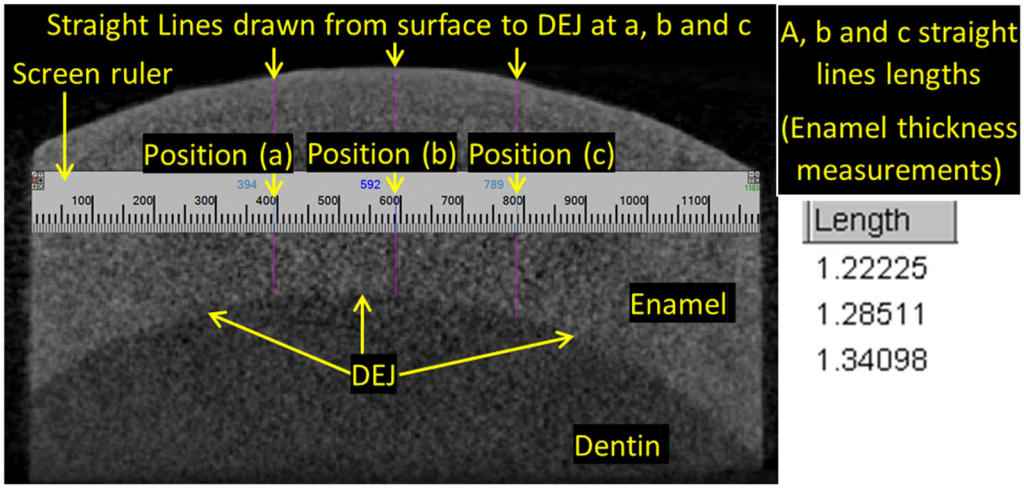

4.3. Results

3.3.1. Thickness measurement of natural-surface enamel by CP-OCT and Micro-CT

The mean of enamel thickness measurements for natural surface enamel by CP-OCT did not significantly differ from the mean measurements by micro-CT (p-value= 0.30). There was excellent agreement between CP-OCT and micro-CT for thickness measurement of natural-surface enamel (ICC 0.98, Table 4.1).

4.3.2. Thickness measurement of worn enamel

Following enamel wear, the mean of enamel thickness measurements by CP-OCT did not significantly differ from the mean measurements by micro-CT (p-value= 0.39). There was an excellent agreement between CP-OCT and micro-CT for thickness measurement of worn enamel (ICC 0.99, Table 4.1). A Bland-Altman plot (Figure 4.3) did not show a specific pattern of disagreement between the two methods and shows an agreement limit of approx. ± 0.10 mm.

Among wear stages, there were significant differences in enamel thickness measurements between all wear stages for both methods, the micro-CT and CP-OCT (p-value<0.0001 for all; Table 4.2).

4.3.3. Wear depth estimation

The estimated wear depth measurements at each wear stage compared to wear 1 are presented in Table 4.2. There were significant differences in wear depths between all wear stages for both methods, the micro-CT and CP-OCT (p-value<0.0001 for all). The mean of wear depth measurements by CP-OCT did not significantly differ from the mean measurements by micro-CT (p-value= 0.87; Table 4.3). There was a good agreement between CP-OCT and micro-CT for wear depth estimation (ICC 0.77, Table 4.3). A Bland-Altman plot (Figure 4.4) did not show a specific pattern of disagreement between the two methods for wear depth estimation and shows agreement limits of approx. ± 0.12 mm.

Table 4.1. Enamel thickness (mean ± standard error and range, in mm) by CP-OCT and micro-CT obtained at baseline (natural surface) and following enamel wear.

Enamel Thickness	CP-OCT		Micro-CT		CP-OCT vs. micro-CT	
	Mean±SE	Range	Mean±SE	Range	p-value	ICC
Natural surface	1.40±0.05	0.81-1.81	1.39±0.05	0.81-1.83	0.30	0.98
Worn surface	1.08±0.02	0.38-1.64	1.09±0.02	0.35-1.71	0.39	0.99

ICC, Intraclass Correlation Coefficient; SE, Standard Error

Table 4.2. Comparison of enamel thickness measurements and wear depth measurements among wear stages.

Wear stage	CP-OCT				Micro-CT			
	Enamel Thickness		Wear depth*		Enamel Thickness		Wear depth*	
	Mean±SD	Range	Mean±SD	Range	Mean±SD	Range	Mean±SD	Range
Wear 1	1.19±0.28 [a]	0.56-1.64	---	---	1.20±0.26 [a]	0.71-1.67	---	---
Wear 2	1.15±0.28 [b]	0.55-1.59	0.04±0.03 [a]	-0.03-0.09	1.16±0.28 [b]	0.60-1.71	0.04±0.05 [a]	-0.05-0.16
Wear 3	1.09±0.27 [c]	0.53-1.58	0.10±0.03 [b]	0.03-0.16	1.09±0.27 [c]	0.53-1.57	0.10±0.05 [b]	0.02-0.23
Wear 4	1.03±0.29 [d]	0.43-1.55	0.17±0.04 [c]	0.06-0.25	1.03±0.28 [d]	0.47-1.52	0.16±0.06 [c]	0.06-0.29
Wear 5	0.95±0.27 [e]	0.38-1.42	0.24±0.03 [d]	0.19-0.32	0.96±0.28 [e]	0.35-1.51	0.24±0.05 [d]	0.16-0.41

*SD, Standard Deviation. The different uppercase letters within mean±SD column indicate significant difference (p-value<0.0001); * Enamel thickness subtracted from Wear 1*

Table 4.3. Mean ± standard error and range of wear depth measurements (estimated following Wear 2, 3 ,4 and 5) in mm by CP-OCT and micro-CT with a p-value of inter-method measurements difference and intra-class correlation coefficient value.

Wear depth	CP-OCT		Micro-CT		CP-OCT vs. micro-CT	
	Mean±SE	Range	Mean±SE	Range	p-value	ICC
Wear 2 to Wear 5	0.14 ±0.01	-0.03-0.32	0.14±0.01	-0.05-0.41	0.87	0.77

SE, Standard Error

Figure 4.3. Bland-Altman plot representing the mean (in X-axis) and the difference (in Y-axis) between micro-CT and CP-OCT enamel thickness measurements pairs.

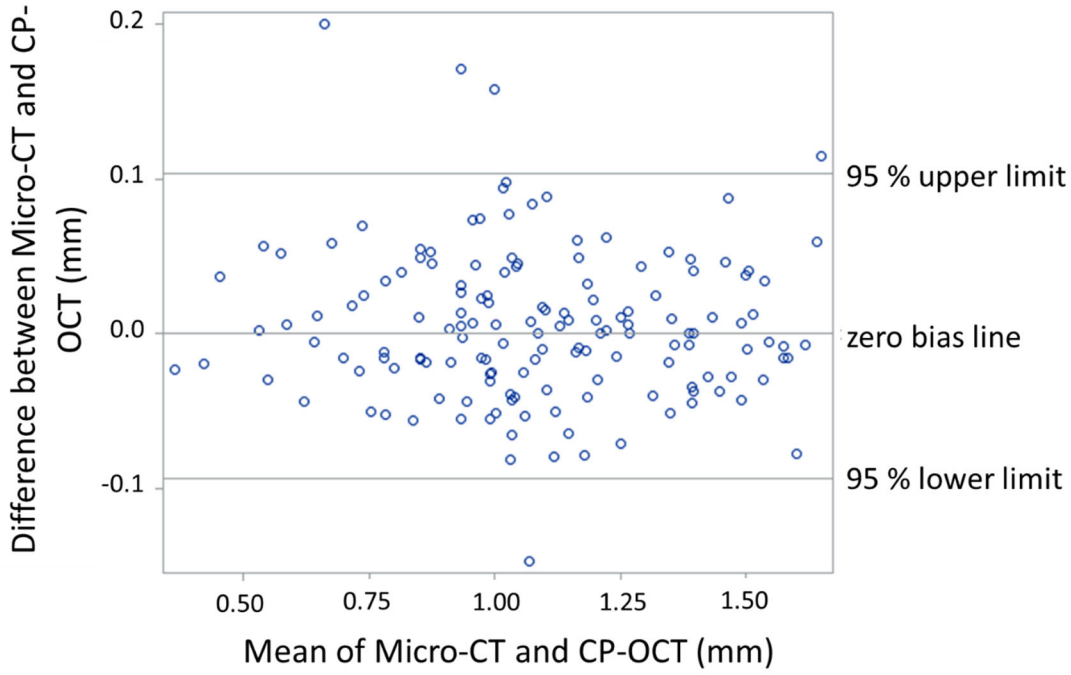

Figure 4.4. Bland-Altman plot representing the mean (in X-axis) and the difference (in Y-axis) between micro-CT and CP-OCT wear depth measurements pairs.

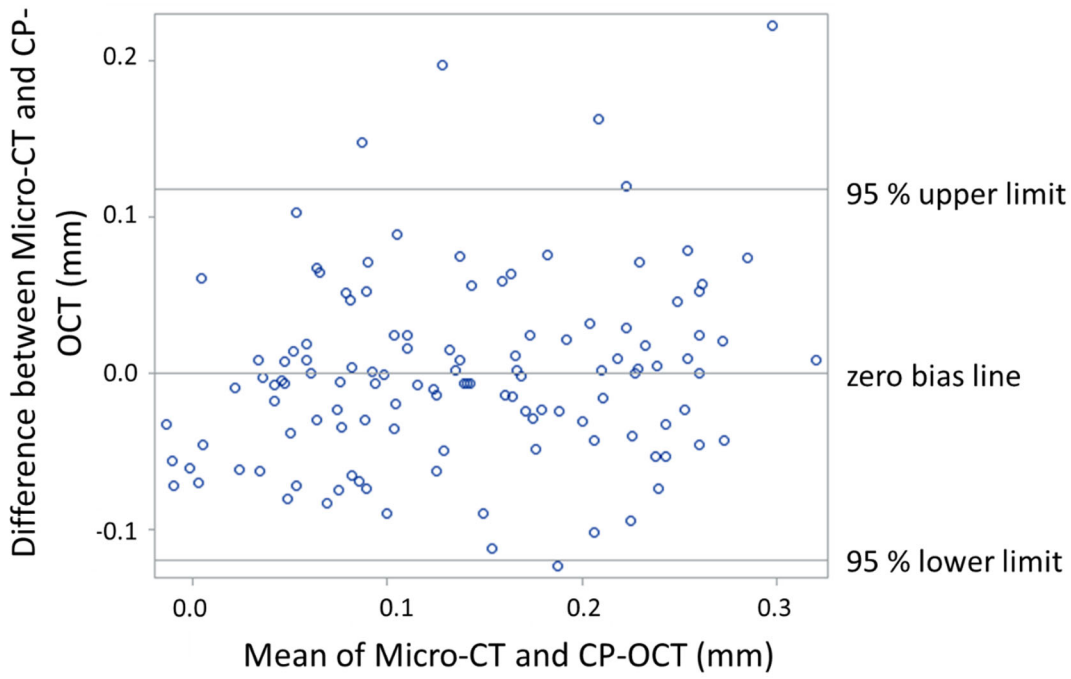

4.4. Discussion

In the present in vitro study, I evaluated the effect of natural and worn enamel surfaces on enamel thickness measurements by CP-OCT, and assessed the capability of CP-OCT to monitor simulated incremental enamel wear.

As the DEJ landmark was identified in all CP-OCT scans, I was able to obtain measurements in all specimens with natural surface enamel. CP-OCT also allowed us to identify a wide range of enamel thicknesses, ranging from 0.81 mm to as high as 1.81 mm.

CP-OCT measurements of enamel thickness with natural unpolished surface agreed very well with the measurements by micro-CT. Both methods yielded nearly similar measurement means and they exhibited an excellent ICC value. My findings also

support the fact that the optical penetration of cross-polarization images of polarization-sensitive OCT device is unaffected by surface topography of the tooth, which is in agreement with Jones et al. (2006). My results indicate that natural enamel surface did not impact the enamel thickness measurement by CP-OCT and support the use of CP-OCT for an accurate baseline evaluation of enamel thickness.

OCT along with ultrasonography are in vivo non-invasive imaging technologies that work by the same principle of utilizing non-ionizing radiation (light and sound, respectively) and by analyzing the back-reflected waves from the examined tissues to construct structural images. Their ability to determine enamel thickness has shown to be encouraging. Ultrasound measurements of enamel thickness showed an excellent agreement with histology (ICC of 0.97, Bland-Altman plot limits of agreement from -0.17 to 0.21 mm) (Sindi et al., 2015). However, the curvature of the natural enamel surface and the DEJ, whether on occlusal or smooth surfaces of teeth, pose a challenge in ultrasound probe positioning and imaging (Huysmans and Thijssen, 2000, Louwerse et al., 2004, Tagtekin et al., 2005; Hughes et al., 2009; Sindi et al, 2015).

On the other hand, my study shows that the natural curvature in the smooth surfaces of molars did not affect the measurements by CP-OCT.

CP-OCT also allowed enamel thickness measurement after wear simulation. I were able to measure the thickness in all worn specimens, ranging from 0.38 to 1.64 mm. These findings are consistent with the findings obtained for sound flattened enamel (Algarni et al., 2016). There was an excellent agreement between the thickness measurements of worn enamel by CP-OCT and the measurements by the gold-standard method. Based on the inter-method agreement analysis, the performance of CP-OCT in

the current study for enamel thickness measurement seems to be superior to the co-polarization OCT imaging reported in a previous study (Algarni et al., 2016). The difference in mean measurements was significant between co-polarization OCT and micro-CT (0.06±0.02 mm; ICC of 0.95) (Algarni et al., 2016), whereas the difference was not significant between standard method and CP-OCT in the current study (0.01±0.01 mm, ICC of 0.95).

CP-OCT was able to monitor enamel thickness along the five stages, as the measurements were decreasing with wear progression. Also, CP-OCT was able to differentiate the thickness at each wear stage from the other stages as exhibited by significant differences in measurements among wear stages, which was comparable to the micro-CT findings (Table 4.2).

The magnitude of incremental wear I created in this study allowed us to evaluate the ability of the CP-OCT to detect the small wear changes. The CP-OCT wear depth measurements were comparable to the measurements by micro-CT, which ranged from 0.04±0.03 mm to 0.24±0.03 mm. This similarity in measurements between the two methods was also evidenced by the good inter-method agreement (ICC of 0.77). The significant differences I found in CP-OCT wear depth measurements among and between the wear stages indicate that CP-OCT allowed differentiation of small changes in wear depth between each wear stage. Despite the accurate measurements by CP-OCT, the method presented low measurement precision for wear depth measurements compared to micro-CT, as depicted from the limits of agreement (approximately ±0.12 mm) in the Bland-Altman plot (Figure 4.4).

There is limited information on the ability of OCT to quantify enamel thickness changes by wear smaller than 0.1 mm. Kim et al. (2017) used OCT as a gold-standard to evaluate QLF's ability to measure occlusal enamel thickness measured every 100 μm. Oguro et al. (2016) used OCT to measure enamel thickness of labial surfaces of incisors following serial enamel trimming by approximately 100 μm for evaluation of enamel thickness effect on the tooth color. Because OCT performance was not the main focus in these studies, there was no information on the challenges encountered or the limitations observed with enamel thickness measurement by OCT.

In the current study, I demonstrated that using the DEJ on an OCT image as a reference is a suitable approach for quantifying and monitoring enamel thickness changes. This method involves scanning the area directly on the tooth, thus it eliminates the problem of dimensional changes with impressions in an indirect tooth wear analysis (Rodriguez and Bartlett, 2011). The CP-OCT results in my study compared well with micro-CT, the most appropriate non-destructive method available to date for enamel thickness measurement. This method allows the output 2D images to be viewed on any plane from a 3D image, like viewing and obtaining OCT b-scans. Micro-CT was used for the same purpose in many in vitro studies focusing on clinical and anthropological applications (Suwa and Kono, 2005; Olejniczak and Grine, 2005; Olejniczak and Grine, 2006; Algarni et al., 2016). It is noteworthy that the wear depth measurements utilizing CP-OCT exhibited lower variability than those with micro-CT, which can be interpreted as a superior performance of CP-OCT for wear depth estimation. A possible source of discrepancy in measurements for both micro-CT and CP-OCT may be errors in the localization of the measurement position and the DEJ landmark, as noted in Chapter 2.

This study evaluated the performance of CP-OCT on smooth surfaces of molars; thus, the results can be projected clinically to the accessible smooth surfaces of teeth only. It is still necessary to verify that results would be similar on more complicated topographies, such as the occlusal and incisal tooth surfaces. Besides, it is still not known whether the change in the probe angulation, which may be necessary for scanning lingual surfaces of teeth, would affect the quality of the scans and measurements. Since I have tested the performance CP-OCT under a controlled specimen hydration condition, the degree of teeth hydration is another aspect that need to be evaluated to ensure the usefulness of the method in the variable hydration environment intraorally. It was evident from the previous studies that enamel surface roughening with the silicon carbide grinding papers (Chapter 2) and pumice prophylaxis (Ravichandran et al., 2019) did not affect the CP-OCT enamel thickness measurement. Further testing involving enamel wear combined with other intra-oral aspects, such as dental pellicle, on the clinical monitoring of ETW by CP-OCT would allow the better understanding of this method's capabilities and limitations.

The performance of the tested method indicates that it can be a viable option to clinically monitor enamel wear longitudinally for patients at high risk of tooth wear.

In conclusion, CP-OCT allows accurate measurement of enamel thickness on natural tooth surfaces. Enamel thickness measurement by CP-OCT allows quantitative monitoring of enamel thickness changes and wear depth following progressive wear.

CHAPTER 5: GENERAL DISCUSSION AND CONCLUSIONS

My long-term goal is to develop an objective method for the clinical assessment and monitoring of ETW. Most of the available methods rely on the comparison between the lesion area and the surrounding sound tooth surface. However, ensuring a stable surface reference point for long term assessment in a non-invasive manner is nonviable because progressing ETW lesions become broader and deeper, and the entire surface of the tooth may become affected at advanced stages. In addition, the poorly defined borders of the lesions make initial identification of intact surfaces difficult, especially in their early stages. The approach proposed in this project can indeed overcome this issue because it employs the DEJ as a reference point for measuring the enamel thickness, thus serving as a consistent measurement landmark over time (Wilder-Smith et al., 2009; Chan et al., 2013). To ensure the usefulness of this approach, I evaluated the influence of different enamel surface micromorphologies and different depths of ETW on CP-OCT enamel thickness measurements in addition to the method's ability to monitor progressing lesions over time.

In Chapter 2, I tested the ability of CP-OCT to estimate and monitor surface loss of enamel with varying degrees of surface roughness following 1, 2, 4, 6, 8, 16 and 24 h of dental erosion. The accuracy of the method was evaluated using measurements by optical profilometry, a highly sensitive gold standard laboratory method for measuring enamel surface loss. CP-OCT performed equally in all degrees of surface roughness, from very rough to smooth enamel surfaces. However, the method did not allow reliable detection of enamel surface loss of less than ~70 μm, which was smaller than the estimated error of the measurement method. Another drawback observed in this study

was the lack of visualization of the DEJ in some scans, as noted also by Chan et al. (2013). On the other hand, the enamel thickness measurement method using CP-OCT was repeatable, as shown from the results on intra-examiner repeatability.

In Chapter 3, I demonstrated the ability of CP-OCT to quantify enamel thickness in the presence and absence of clinically-relevant surface erosion at different degrees of enamel surface roughness and wear depths. Its capability to quantify enamel thickness following dental erosion was further supported by the high agreement with the measurements by micro-CT. In addition, I showed the ability of this approach to differentiate enamel wear depth of approximately 300 µm and 500 µm under the simulated enamel surface erosion, roughness, and wear conditions. In this study, the ability of the CP-OCT to show the DEJ was superior to its performance observed in Chapter 2 and in the study by Chan et al. (2013), where prolonged dental erosion challenges were carried out. Thus, it can be inferred that CP-OCT allows the measurement of enamel thickness in sound enamel and also on enamel exposed to a clinically relevant dental erosion challenge. However, the device's ability to reveal the DEJ landmark for enamel thickness measurement becomes unpredictable following 1 h of dental erosion.

The Chapter 4 study demonstrated the ability of CP-OCT to quantify enamel thickness on the natural surface for the first time. Also, the ability of CP-OCT to identify wear depths demonstrated in Chapter 3 was further explored in the Chapter 4 study by evaluating its ability to differentiate wear depths of at least 50 µm, which has not been explored before. The accuracy of the enamel thickness and wear depth measurements by CP-OCT was evaluated and supported using measurements by micro-CT, a sensitive,

non-destructive gold standard method for in vitro enamel thickness determination (see the Appendix). From the results of Chapter 4, I suggest that CP-OCT can be an accurate and usable clinical method to measure and monitor enamel thickness in curved smooth enamel surface undergoing progressive wear.

Based on what I have learned from the results of this project, CP-OCT offers remarkable clinical applications. Using this method, monitoring enamel thickness undergoing ETW can be achieved with high accuracy (Chapters 2 and 4) and repeatability (Chapter 2). Additionally, the method allowed estimation of enamel thickness loss of more than 50 μm. ETW assessment using this method can conveniently be performed chairside without the hassle of taking impressions, fabricating study models, and analyzing and storing them for follow-up comparisons. The CP-OCT method is particularly helpful for longitudinal evaluation of teeth in patients at a high risk of developing ETW, such as those suffering from exposure of teeth to gastric acids due to gastroesophageal reflux disease (GERD) or eating disorders. In high-risk groups, tooth surfaces can lose from approximately 80-160 μm per year (Bartlett et al., 1997) to as high as 217 μm over a 6-month period as reported in one case by Rodriguez et al. (2012). For that, CP-OCT could provide a practical and meticulous assessment method of enamel loss clinically on a regular basis for patients at high ETW risk.

This dissertation expands the knowledge of the capabilities and limitations of CP-OCT for measuring enamel loss and monitoring ETW. I expect it to positively impact the oral healthcare field by providing a scientific basis for CP-OCT use to objectively monitor ETW in clinical studies and clinical practice.

In this project, I proposed and explored the use of an advanced dental OCT system (CP-OCT) for enamel thickness measurement and surface loss/wear depth estimation to objectively quantify and monitor ETW. I simulated the conditions of ETW in vitro to test the effects of dental erosion severities, surface roughness, wear degrees, and curvature of natural tooth surface under controlled conditions. From my findings, I can conclude the following:

Chapter 2: Enamel surface roughness, in the presence of dental erosion demineralization, did not affect enamel surface loss estimation by CP-OCT. CP-OCT allowed repeatable enamel surface loss estimation for the majority of specimens during and following prolonged progressive dental erosion challenges from 1 h to 24 h. However, CP-OCT's ability to quantify the surface loss was dictated by its ability to show the DEJ in the scans for enamel thickness measurement, which was unpredictable. Moreover, the method's measurement error substantially limits the accurate estimation of dental erosion enamel surface loss of less than 70 μm.

Chapter 3: Enamel surface roughness and the presence of dental erosion did not affect enamel thickness measurements by CP-OCT. CP-OCT allowed enamel thickness determination equally on either thinner or thicker enamel (eroded for 10 min or non-eroded). It also differentiated the simulated enamel wear levels.

Chapter 4: CP-OCT accurately allowed thickness measurement of enamel with either a natural- or worn-surface. It also allowed monitoring of enamel thickness and estimation of wear depths following simulated wear.

APPENDIX

Table A.1. Methods for enamel thickness measurement

Method	Example studies	Advantages	Disadvantages
Radiography (periapical, bitewing and lateral)	Alvesalo and Tammisalo, 1981(1); Stroud et al., 1994 (2); Harris and Hicks, 1998 (3); Grine et al., 2001(4); Ang et al., 2017 (5)	• Non-destructive • In vivo and in vitro imaging • Readily available for routine dental exam	• Provide only 2D representation of tooth (6) • limited accuracy (4) • Ionizing radiation exposure (6) • Image size/shape distortion (7) and angulation issues (5)
Optical coherence tomography (OCT)	Wilder-Smith et al., 2009 (8); Chan et al., 2013 (9); Algarni et al., 2016 (10); Machoy et al., 2018 (11); Alghilan et al., 2019 (12)	• Non-destructive • In vivo and in vitro imaging • No ionizing radiation used • Real-time 1D, 2D, and 3D imaging • Highly agreed with histology and Micro-CT (10) • High sensitivity • Portable • Low cost (6)	• Small scanning area (few millimeters) and limited penetration depth (3 mm) (6) • Not widely commercially available (13)
Computed tomography (CT)	Grine, 1991(14); Spoor et al., 1993 (15)	• Non-destructive • In vivo and in vitro imaging • Provide axial cross-sectional scans, which can be viewed in axial, sagittal and coronal planes (16) • 3D images can be generated using computer programs (16)	• Ionizing radiation exposure • Not indicated for routine dental care • Inaccurate measurement of enamel thickness due to limited spatial resolution (14) • Thin enamel cannot be visualized and measured (14, 15, 17) • High cost

Cone beam computed tomography (CBCT)	Brokos et al., 2015 (18)	• Non-destructive • In vivo and in vitro imaging • Provides 2D, and 3D images viewed from any plane (16) • Lower radiation dose and cost than conventional CT (16) • Better hard tissues resolution than conventional CT (18) • Comparable to Micro-CT for volumetric measurement and dentin thickness (19-21) • Availability in many dental clinics (18)	• Ionizing radiation exposure • Not indicated for routine dental care • Image sharpness affected by patient motion (heartbeat and breathing) and partial-volume effect artifact (18, 22) • High cost
X-ray Micro-computed tomography (Micro-CT)	Sua and Kono, 2005 (23); Olejniczak and Grine, 2005 (24); Olejniczak and Grine, 2006 (17); Algarni et al., 2016 (10)	• Non-destructive • In vivo for small animals and in vitro imaging (25) • Provides 2D, and 3D images with high resolution (25) • Allow accurate enamel thickness measurement (24) • Allows detecting very small changes in enamel volume (25) • Faster processing time than histological methods (25)	• For human teeth, available only for in vitro evaluation • Ionizing radiation exposure • Difficulty in visualizing very thin enamel areas (less than 0.01mm) in raw Micro-CT images of highly mineralized teeth (17)
Ultrasonography	Barber and Lobene, 1969 (26); Ng et al., 1989 (27); Huysmans and Thijssen, 2000 (28); Louwerse et al., 2004 (29); Tagtekin et al., 2005 (30); Dwyer-Joyce et	• Non-destructive • In vivo and in vitro imaging • No ionizing radiation used • Real-time 1D, 2D, and 3D imaging • Highly agreed with histology (35) • Portable	• Produce unreliable measurements in curved enamel surfaces (35) and thin enamel of less than or about 0.5 mm thick (28) • Can not reliably detect enamel changes less than 0.12 mm (33) or even less than 0.33 mm (29) • Difficult repositioning of the probe causes poor measurement repeatability (28, 29, 33) • Large beam diameter cause uncertainty in the measurement position (26)

	al., 2010 (31); Harput et al., 2011 (32); Slak et al., 2011 (33); Sindi et al., 2014 (34); Sindi et al., 2015 (35)		• Require a coupling medium and contact between the transducer tip and tooth surface (28, 30) • Probe may slightly displaced on enamel covered with coupling agent, which cause measurement variability (28, 33) • Necessitate moving the probe several times until a satisfactory waveform is obtained (30, 31) • Ultrasonic velocity is affected by enamel prism orientation (27, 32, 33) • Probe's angulation, deviation from perpendicular position, causes unknown measurement variation (29) and loss of DEJ signal (31) • Weak echo signal in areas with curved DEJ as incisal surface (34)
Micrograph or macrophotograph of physical cross-section	Olejniczak and Grine, 2006 (17); Smith et al., 2006 (36); Mahoney et al., 2010 (37)	• Allow accurate enamel thickness measurement in a particular section (17) • Data on enamel thickness using histology are widely available (36)	• Destructive and causes irreversible damage (17) • Does not allow longitudinal monitoring of the examined tooth area (38) • Provide only 2D image (25, 37) • Only for in vitro evaluation • Difficult to precisely locate and obtain the section of a specific site (39) • Small details in specimen may be lost during processing of the cut site (39, 40) • High chance of loosing the specimens during sectioning process (41), thus using the method for studies may require large number of samples • Require sample processing, which is time consuming (40)

1.(Alvesalo and Tammisalo, 1981); 2.(Stroud et al., 1994); 3.(Harris and Hicks, 1998); 4.(Grine et al., 2001); 5.(Ang et al., 2017); 6.(Hsieh et al., 2013); 7.(White and Pharoah, 2004); 8.(Wilder-Smith et al., 2009); 9.(Chan et al., 2013); 10.(Algarni et al., 2016); 11.(Machoy et al., 2018); 12.(Alghilan et al., 2019); 13.(Katkar et al., 2018); 14.(Grine, 1991); 15.(Spoor et al., 1993); 16.(Frederiksen, 2004); 17.(Olejniczak and Grine, 2006); 18.(Brokos et al., 2015); 19.(Wang et al., 2011); 20.(Maret et al., 2010); 21.(Xu et al., 2017); 22.(Ye et al., 2012); 23.(Suwa and Kono, 2005); 24. (Olejniczak and Grine, 2005); 25.(Dong et al., 2014); 26.(Barber et al., 1969); 27.(Ng et al., 1989); 28.(Huysmans and Thijssen, 2000); 29.(Louwerse et al., 2004); 30.(Tagtekin et al., 2005); 31.(Dwyer-Joyce

et al., 2010); 32.(Harput et al., 2011); 33.(Slak et al., 2011); 34.(Sindi et al., 2014) 35.(Sindi et al., 2015); 36.(Smith et al., 2006); 37.(Mahoney, 2010); 38.(Soviero et al., 2012); 39.(Huysmans and Longbottom, 2004); 40.(Ricketts et al., 1998); 41.(Rhodes et al., 1999)

REFERENCES

Aden A, Anthony A, Brigi C, Merchant MS, Siraj H, Tomlins PH: Dynamic measurement of the optical properties of bovine enamel demineralization models using four-dimensional optical coherence tomography. J Biomed Opt 2017;22:76020.

Agrawal A, Chen CW, Baxi J, Chen Y, Pfefer TJ: Multilayer thin-film phantoms for axial contrast transfer function measurement in optical coherence tomography. Biomed Opt Express 2013;4:1166-1175.

Al-Dlaigan YH, Al-Meedania LA, Anil S: The influence of frequently consumed beverages and snacks on dental erosion among preschool children in Saudi Arabia. Nutrition journal 2017;16:80.

Al-Majed I, Maguire A, Murray JJ: Risk factors for dental erosion in 5–6 year old and 12–14 year old boys in Saudi Arabia. Community dentistry and oral epidemiology 2002;30:38-46.

Al-Malik MI, Holt RD, Bedi R: Erosion, caries and rampant caries in preschool children in Jeddah, Saudi Arabia. Community Dentistry and Oral Epidemiology 2002;30:16-23.

Algarni A, Kang H, Fried D, Eckert GJ, Hara AT: Enamel Thickness Determination by Optical Coherence Tomography: In vitro Validation. Caries Res 2016;50:400-406.

Alghilan MA, Lippert F, Platt JA, Eckert GJ, Gonzalez-Cabezas C, Fried D, Hara AT: Impact of surface micromorphology and demineralization severity on enamel loss measurements by cross-polarization optical coherence tomography. J Dent 2019;81:52-58.

Alvesalo L, Tammisalo E: Enamel thickness of 45,X females' permanent teeth. Am J Hum Genet 1981;33:464-469.

Amaechi BT: Assessment and monitoring of dental erosion; in: Dental Erosion and Its Clinical Management. Springer, 2015, pp 111-119.

Amaechi BT, Higham SM: In vitro remineralisation of eroded enamel lesions by saliva. J Dent 2001;29:371-376.

Amaechi BT, Higham SM, Podoleanu AG, Rogers JA, Jackson DA: Use of optical coherence tomography for assessment of dental caries: quantitative procedure. Journal of oral rehabilitation 2001;28:1092-1093.

Anderson P, Creanor S: Enamel; in Creanor S (ed): Essential Clinical Oral Biology. Chichester, West Sussex, UK, Wiley Blackwell, 2016, pp 23-33.

Ang AG, Steegmans PA, Kerdijk W, Livas C, Ren Y: Radiographic technique and brackets affect measurements of proximal enamel thickness on mandibular incisors. Eur J Orthod 2017;39:25-30.

Austin RS, Haji Taha M, Festy F, Cook R, Andiappan M, Gomez J, Pretty IA, Moazzez R: Quantitative Swept-Source Optical Coherence Tomography of Early Enamel Erosion in vivo. Caries Res 2017;51:410-418.

Baek JH, Krasieva T, Tang S, Ahn Y, Kim CS, Vu D, Chen Z, Wilder-Smith P: Optical approach to the salivary pellicle. J Biomed Opt 2009;14:044001.

Barber F, Lees S, Lobene R: Ultrasonic pulse-echo measurements in teeth. Archives of oral biology 1969;14:745-IN743.

Bartlett D, Ganss C, Lussi A: Basic Erosive Wear Examination (BEWE): a new scoring system for scientific and clinical needs. Clinical oral investigations 2008;12:65-68.

Bartlett DW: Retrospective long term monitoring of tooth wear using study models. Br Dent J 2003;194:211-213; discussion 204.

Bartlett DW, Blunt L, Smith BG: Measurement of tooth wear in patients with palatal erosion. Br Dent J 1997;182:179-184.

Baumgartner A, Dichtl S, Hitzenberger C, Sattmann H, Robl B, Moritz A, Fercher A, Sperr W: Polarization–sensitive optical coherence tomography of dental structures. Caries research 2000;34:59-69.

Brokos Y, Stavridakis M, Bortolotto Ibarra T, Krejci I: Evaluation of enamel thickness of upper anterior teeth in different age groups by dental cone beam computed tomography scan in vivo. International Journal of Advances in Case Reports 2015;2:1396-1409.

Carvalho T, Colon P, Ganss C, Huysmans M, Lussi A, Schlüter N, Schmalz G, Shellis RP, Tveit A, Wiegand A: Consensus report of the European Federation of Conservative Dentistry: erosive tooth wear—diagnosis and management. Clinical oral investigations 2015;19:1557-1561.

Chan KH, Chan AC, Darling CL, Fried D: Methods for Monitoring Erosion Using Optical Coherence Tomography. Proc SPIE Int Soc Opt Eng 2013;8566:856606.

Chan KH, Tom H, Darling CL, Fried D: A method for monitoring enamel erosion using laser irradiated surfaces and optical coherence tomography. Lasers Surg Med 2014;46:672-678.

Chan KH, Tom H, Lee RC, Kang H, Simon JC, Staninec M, Darling CL, Pelzner RB, Fried D: Clinical monitoring of smooth surface enamel lesions using CP-OCT during nonsurgical intervention. Lasers Surg Med 2016;48:915-923.

Chew HP, Zakian CM, Pretty IA, Ellwood RP: Measuring initial enamel erosion with quantitative light-induced fluorescence and optical coherence tomography: an in vitro validation study. Caries Res 2014;48:254-262.

Chong SL, Darling CL, Fried D: Nondestructive measurement of the inhibition of demineralization on smooth surfaces using polarization-sensitive optical coherence tomography. Lasers Surg Med 2007;39:422-427.

Chung S, Fried D, Staninec M, Darling CL: Multispectral near-IR reflectance and transillumination imaging of teeth. Biomed Opt Express 2011;2:2804-2814.

Colston BW, Sathyam US, DaSilva LB, Everett MJ, Stroeve P, Otis L: Dental oct. Optics express 1998;3:230-238.

Darling CL, Huynh G, Fried D: Light scattering properties of natural and artificially demineralized dental enamel at 1310 nm. Journal of biomedical optics 2006;11:034023.

Dong G, Dong Q, Liu Y, Lou B, Feng J, Wang K, Zhou X, Wu H: High-resolution micro-CT scanning as an innovative tool for evaluating dental hard tissue development. Journal of applied clinical medical physics 2014;15:335-344.

Dwyer-Joyce RS, Goodman MA, Lewis R: A comparative study of ultrasonic direct contact, immersion, and layer resonance methods for assessment of enamel thickness in teeth. Proceedings of the Institution of Mechanical Engineers, Part J: Journal of Engineering Tribology 2010;224:519-528.

El Wazani B, Dodd M, Milosevic A: The signs and symptoms of tooth wear in a referred group of patients. British dental journal 2012;213:E10.

Everett MJ, Colston BW, Sathyam US, Da Silva LB, Fried D, Featherstone JD: Noninvasive diagnosis of early caries with polarization-sensitive optical coherence tomography (PS-OCT); in: Lasers in dentistry V. International Society for Optics and Photonics, 1999, vol 3593, pp 177-183.

Field J, Waterhouse P, German M: Quantifying and qualifying surface changes on dental hard tissues in vitro. J Dent 2010;38:182-190.

Frederiksen N: Specialized radiographic techniques in oral radiology; Principles and interpretation. White SC, Pharoah MJ 2004;5:262-263.

Fried D, Glena RE, Featherstone JD, Seka W: Nature of light scattering in dental enamel and dentin at visible and near-infrared wavelengths. Applied optics 1995;34:1278-1285.

Fried D, Xie J, Shafi S, Featherstone JD, Breunig TM, Le C: Imaging caries lesions and lesion progression with polarization sensitive optical coherence tomography. J Biomed Opt 2002;7:618-627.

Fujimoto JG, Drexler W: Introduction to OCT; in Drexler W, Fujimoto JG (eds): Optical Coherence Tomography: Technology and Applications. Cham, Springer International Publishing, 2015, pp 3-64.

Ganss C: Is erosive tooth wear an oral disease? Monographs in oral science 2014;25:16-21.

Ganss C, Klimek J, Giese K: Dental erosion in children and adolescents–a cross-sectional and longitudinal investigation using study models. Community Dentistry and Oral Epidemiology 2001;29:264-271.

Ganss C, Klimek J, Lussi A: Accuracy and consistency of the visual diagnosis of exposed dentine on worn occlusal/incisal surfaces. Caries research 2006;40:208-212.

Ganss C, Lussi A, Schlueter N: The histological features and physical properties of eroded dental hard tissues; in: Erosive tooth wear. Karger Publishers, 2014, vol 25, pp 99-107.

Grine FE: Computed tomography and the measurement of enamel thickness in extant hominoids: implications for its palaeontological application. Palaeontol Africana 1991;28: 61-69.

Grine FE, Stevens NJ, Jungers WL: An evaluation of dental radiograph accuracy in the measurement of enamel thickness. Arch Oral Biol 2001;46:1117-1125.

Hariri I, Sadr A, Nakashima S, Shimada Y, Tagami J, Sumi Y: Estimation of the enamel and dentin mineral content from the refractive index. Caries Res 2013;47:18-26.

Harput S, Evans T, Bubb N, Freear S: Diagnostic ultrasound tooth imaging using fractional fourier transform. IEEE transactions on ultrasonics, ferroelectrics, and frequency control 2011;58.

Harris EF, Hicks JD: A radiographic assessment of enamel thickness in human maxillary incisors. Arch Oral Biol 1998;43:825-831.

Hsieh Y-S, Ho Y-C, Lee S-Y, Chuang C-C, Tsai J-c, Lin K-F, Sun C-W: Dental optical coherence tomography. Sensors 2013;13:8928-8949.

Hsieh YS, Ho YC, Lee SY, Lu CW, Jiang CP, Chuang CC, Wang CY, Sun CW: Subgingival calculus imaging based on swept-source optical coherence tomography. J Biomed Opt 2011;16:071409.

Huang D, Swanson EA, Lin CP, Schuman JS, Stinson WG, Chang W, Hee MR, Flotte T, Gregory K, Puliafito CA, et al.: Optical coherence tomography. Science 1991;254:1178-1181.

Hughes D, Girkin J, Poland S, Longbottom C, Button T, Elgoyhen J, Hughes H, Meggs C, Cochran S: Investigation of dental samples using a 35 MHz focussed ultrasound piezocomposite transducer. Ultrasonics 2009;49:212-218.

Huysmans M, Thijssen J: Ultrasonic measurement of enamel thickness: a tool for monitoring dental erosion? Journal of dentistry 2000;28:187-191.

Huysmans MC, Chew HP, Ellwood RP: Clinical studies of dental erosion and erosive wear. Caries Res 2011;45 Suppl 1:60-68.

Huysmans MC, Longbottom C: The challenges of validating diagnostic methods and selecting appropriate gold standards. J Dent Res 2004;83 Spec No C:C48-52.

Imfeld T: Dental erosion. Definition, classification and links. Eur J Oral Sci 1996;104:151-155.

Jaeggi T, Lussi A: Prevalence, incidence and distribution of erosion; in: Erosive Tooth Wear. Karger Publishers, 2014, vol 25, pp 55-73.

Jager D, Vieira A, Ruben J, Huysmans M: Estimated erosive potential depends on exposure time. Journal of dentistry 2012;40:1103-1108.

Jansonius NM, Cervantes J, Reddikumar M, Cense B: Influence of coherence length, signal-to-noise ratio, log transform, and low-pass filtering on layer thickness assessment with OCT in the retina. Biomed Opt Express 2016;7:4490-4500.

Johansson A-K, Johansson A, Birkhed D, Omar R, Baghdadi S, Carlsson GE: Dental erosion, soft-drink intake, and oral health in young Saudi men, and the development of a system for assessing erosive anterior tooth wear. Acta Odontologica Scandinavica 1996;54:369-378.

Jones RS, Darling CL, Featherstone JD, Fried D: Imaging artificial caries on the occlusal surfaces with polarization-sensitive optical coherence tomography. Caries Res 2006;40:81-89.

Jones RS, Fried D: Remineralization of enamel caries can decrease optical reflectivity. J Dent Res 2006;85:804-808.

Jung W, Zhang J, Chung J, Wilder-Smith P, Brenner M, Nelson JS, Chen Z: Advances in oral cancer detection using optical coherence tomography. IEEE Journal of Selected Topics in Quantum Electronics 2005;11:811-817.

Kaidonis J, Richards L, Townsend G, Tansley G: Wear of human enamel: a quantitative in vitro assessment. Journal of dental research 1998;77:1983-1990.

Katkar RA, Tadinada SA, Amaechi BT, Fried D: Optical Coherence Tomography. Dent Clin North Am 2018;62:421-434.

Kim S-K, Lee H-S, Park S-W, Lee E-S, De Jong EDJ, Jung H-I, Kim B-I: Quantitative light-induced fluorescence technology for quantitative evaluation of tooth wear. Journal of biomedical optics 2017;22:121701.

Kreulen C, Van't Spijker A, Rodriguez J, Bronkhorst E, Creugers N, Bartlett D: Systematic review of the prevalence of tooth wear in children and adolescents. Caries research 2010;44:151-159.

Lambrechts P, Braem M, Vuylsteke-Wauters M, Vanherle G: Quantitative in vivo wear of human enamel. Journal of Dental Research 1989;68:1752-1754.

Loomans B, Opdam N, Attin T, Bartlett D, Edelhoff D, Frankenberger R, Benic G, Ramseyer S, Wetselaar P, Sterenborg B: Severe tooth wear: European consensus statement on management guidelines. J Adhes Dent 2017;19:111-119.

Louie T, Lee C, Hsu D, Hirasuna K, Manesh S, Staninec M, Darling CL, Fried D: Clinical assessment of early tooth demineralization using polarization sensitive optical coherence tomography. Lasers Surg Med 2010;42:738-745.

Louwerse C, Kjaeldgaard M, Huysmans M: The reproducibility of ultrasonic enamel thickness measurements: an in vitro study. Journal of dentistry 2004;32:83-89.

Lu C, Nakamura T, Korach CS: Effective property of tooth enamel: Monoclinic behavior. Journal of biomechanics 2012;45:1437-1443.

Lussi A, Bossen A, Hoschele C, Beyeler B, Megert B, Meier C, Rakhmatullina E: Effects of enamel abrasion, salivary pellicle, and measurement angle on the optical assessment of dental erosion. J Biomed Opt 2012;17:97009-97001.

Lussi A, Schlueter N, Rakhmatullina E, Ganss C: Dental erosion--an overview with emphasis on chemical and histopathological aspects. Caries Res 2011;45 Suppl 1:2-12.

Machoy ME, Koprowski R, Szyszka-Sommerfeld L, Safranow K, Gedrange T, Wozniak K: Optical coherence tomography as a non-invasive method of enamel

thickness diagnosis after orthodontic treatment by 3 different types of brackets. Adv Clin Exp Med 2019;28:211-218.

Mahoney P: Two-dimensional patterns of human enamel thickness on deciduous (dm1, dm2) and permanent first (M1) mandibular molars. archives of oral biology 2010;55:115-126.

Mandurah MM, Sadr A, Shimada Y, Kitasako Y, Nakashima S, Bakhsh TA, Tagami J, Sumi Y: Monitoring remineralization of enamel subsurface lesions by optical coherence tomography. J Biomed Opt 2013;18:046006.

Maret D, Molinier F, Braga J, Peters OA, Telmon N, Treil J, Inglèse J, Cossié A, Kahn J-L, Sixou M: Accuracy of 3D reconstructions based on cone beam computed tomography. Journal of dental research 2010;89:1465-1469.

McGuire J, Szabo A, Jackson S, Bradley TG, Okunseri C: Erosive tooth wear among children in the United States: relationship to race/ethnicity and obesity. Int J Paediatr Dent 2009;19:91-98.

Mulic A, Tveit A, Wang N, Hove L, Espelid I, Skaare A: Reliability of two clinical scoring systems for dental erosive wear. Caries research 2010;44:294-299.

Nakagawa H, Sadr A, Shimada Y, Tagami J, Sumi Y: Validation of swept source optical coherence tomography (SS-OCT) for the diagnosis of smooth surface caries in vitro. J Dent 2013;41:80-89.

Nanci A: structure of the oral tissues; in Nanci A (ed): Ten Cate's oral histology: development, structure, and function. St. Louis, Missouri, Mosby, 2013, pp 1-13.

Nazari A, Sadr A, Campillo-Funollet M, Nakashima S, Shimada Y, Tagami J, Sumi Y: Effect of hydration on assessment of early enamel lesion using swept-source optical coherence tomography. J Biophotonics 2013;6:171-177.

Ng S, Payne P, Cartledge N, Ferguson M: Determination of ultrasonic velocity in human enamel and dentine. Archives of Oral Biology 1989;34:341-345.

Oguro R, Nakajima M, Seki N, Sadr A, Tagami J, Sumi Y: The role of enamel thickness and refractive index on human tooth colour. Journal of dentistry 2016;51:36-44.

Okunseri C, Wong M, Yau T, McGrath C, Szabo A: Erosive Tooth Wear and Beverage Consumption Among US Adults. Journal of Dental Research 2014.

Olejniczak AJ, Grine FE: High-resolution measurement of Neandertal tooth enamel thickness by micro-focal computed tomography. S Afr J Sci 2005;101:219-220.

Olejniczak AJ, Grine FE: Assessment of the accuracy of dental enamel thickness measurements using microfocal X-ray computed tomography. Anat Rec A Discov Mol Cell Evol Biol 2006;288:263-275

Pandya M, Diekwisch TG: Enamel biomimetics—fiction or future of dentistry. International journal of oral science 2019;11:8.

Ravichandran NK, Tumkur Lakshmikantha H, Park HS, Jeon M, Kim J: Analysis of Enamel Loss by Prophylaxis and Etching Treatment in Human Tooth Using Optical Coherence Tomography: An In Vitro Study. J Healthc Eng 2019;2019:8973825.

Rhodes JS, Ford TR, Lynch JA, Liepins PJ, Curtis RV: Micro-computed tomography: a new tool for experimental endodontology. Int Endod J 1999;32:165-170.

Ricketts DN, Watson TF, Liepins PJ, Kidd EA: A comparison of two histological validating techniques for occlusal caries. J Dent 1998;26:89-96.

Rodriguez J, Austin R, Bartlett D: In vivo measurements of tooth wear over 12 months. Caries research 2012;46:9-15.

Rodriguez JM, Bartlett DW: The dimensional stability of impression materials and its effect on in vitro tooth wear studies. Dent Mater 2011;27:253-258.

Schlueter N, Hara A, Shellis RP, Ganss C: Methods for the measurement and characterization of erosion in enamel and dentine. Caries Res 2011;45 Suppl 1:13-23.

Schlueter N, Hardt M, Lussi A, Engelmann F, Klimek J, Ganss C: Tin-containing fluoride solutions as anti-erosive agents in enamel: an in vitro tin-uptake, tissue-loss, and scanning electron micrograph study. Eur J Oral Sci 2009;117:427-434.

Schlueter N, Luka B: Erosive tooth wear–a review on global prevalence and on its prevalence in risk groups. British dental journal 2018;224:364.

Shaw L, Smith AJ: Dental erosion--the problem and some practical solutions. Br Dent J 1999;186:115-118.

Shellis RP, Addy M: The interactions between attrition, abrasion and erosion in tooth wear. Monographs in oral science 2014;25:32-45.

Shemesh H, van Soest G, Wu MK, van der Sluis LW, Wesselink PR: The ability of optical coherence tomography to characterize the root canal walls. J Endod 2007;33:1369-1373.

Shimamura Y, Murayama R, Kurokawa H, Miyazaki M, Mihata Y, Kmaguchi S: Influence of tooth-surface hydration conditions on optical coherence-tomography imaging. J Dent 2011;39:572-577.

Sindi KH, Bubb NL, Evans JA, Gutteridge DL: In vivo reproducibility study of ultrasound for monitoring enamel thickness. Oral surgery, oral medicine, oral pathology and oral radiology 2014;118:126-134.

Sindi KH, Bubb NL, Gutteridge DL, Evans JA: In vitro enamel thickness measurements with ultrasound. Ultrasound in medicine & biology 2015;41:301-308.

Slak B, Ambroziak A, Strumban E, Maev RG: Enamel thickness measurement with a high frequency ultrasonic transducer-based hand-held probe for potential application in the dental veneer placing procedure. Acta Bioeng Biomech 2011;13:65-70.

Smith BG, Knight JK: An index for measuring the wear of teeth. Br Dent J 1984;156:435-438.

Smith TM, Olejniczak AJ, Reid DJ, Ferrell R, Hublin J-J: Modern human molar enamel thickness and enamel–dentine junction shape. Archives of oral biology 2006;51:974-995.

Soviero VM, Leal SC, Silva RC, Azevedo RB: Validity of MicroCT for in vitro detection of proximal carious lesions in primary molars. J Dent 2012;40:35-40.

Spijker AVt, Rodriguez JM, Kreulen CM, Bronkhorst EM, Bartlett DW, Creugers NH: Prevalence of tooth wear in adults. International Journal of Prosthodontics 2009;22.

Spoor CF, Zonneveld FW, Macho GA: Linear measurements of cortical bone and dental enamel by computed tomography: applications and problems. American journal of physical anthropology 1993;91:469-484.

Stroud J, Buschang P, Goaz P: Sexual dimorphism in mesiodistal dentin and enamel thickness. Dentomaxillofacial Radiology 1994;23:169-171.

Sugita I, Nakashima S, Ikeda A, Burrow MF, Nikaido T, Kubo S, Tagami J, Sumi Y: A pilot study to assess the morphology and progression of non-carious cervical lesions. Journal of dentistry 2017;57:51-56.

Suwa G, Kono RT: A micro-CT based study of linear enamel thickness in the mesial cusp section of human molars: reevaluation of methodology and assessment of within-tooth, serial, and individual variation. Anthropological Science 2005;113:273-289.

Tagtekin DA, Öztürk F, Lagerweij M, Hayran O, Stookey G, Yanikoglu FÇ: Thickness measurement of worn molar cusps by ultrasound. Caries research 2005;39:139-143.

Tom H, Chan KH, Darling CL, Fried D: Near-IR image-guided laser ablation of demineralization on tooth occlusal surfaces. Lasers Surg Med 2016;48:52-61.

Wang Y, He S, Yu L, Li J, Chen S: Accuracy of volumetric measurement of teeth in vivo based on cone beam computer tomography. Orthodontics & craniofacial research 2011;14:206-212.

Wetselaar P, Wetselaar-Glas MJ, Koutris M, Visscher CM, Lobbezoo F: Assessment of the amount of tooth wear on dental casts and intra-oral photographs. Journal of oral rehabilitation 2016;43:615-620.

White S, Pharoah M: Projection geometry. Oral radiology: principles and interpretation (5th ed) St Louis, MO: Mosby 2004:91-92.

Wilder-Smith CH, Wilder-Smith P, Kawakami-Wong H, Voronets J, Osann K, Lussi A: Quantification of dental erosions in patients with GERD using optical coherence tomography before and after double-blind, randomized treatment with esomeprazole or placebo. Am J Gastroenterol 2009;104:2788-2795.

Xu J, He J, Yang Q, Huang D, Zhou X, Peters OA, Gao Y: Accuracy of Cone-beam Computed Tomography in Measuring Dentin Thickness and Its Potential of Predicting the Remaining Dentin Thickness after Removing Fractured Instruments. Journal of endodontics 2017;43:1522-1527.

Ye N, Jian F, Xue J, Wang S, Liao L, Huang W, Yang X, Zhou Y, Lai W, Li J: Accuracy of in-vitro tooth volumetric measurements from cone-beam computed tomography. American Journal of Orthodontics and Dentofacial Orthopedics 2012;142:879-887.

Zentner A, Duschner H: Structural changes of acid etched enamel examined under confocal laser scanning microscope. J Orofac Orthop 1996;57:202-209.

CURRICULUM VITAE

Maryam Abdulkareem Alghilan

Education

2014-2019 Doctor of Philosophy (Ph.D.) in Dental Sciences, Indiana University School of Dentistry, Indiana University-Purdue University, Indianapolis, Indiana, USA

2012-2014 Master of Science in Dentistry (MSD) in Operative Dentistry, Indiana University School of Dentistry, at Indiana University-Purdue University, Indianapolis, Indiana, USA

2004-2011 Bachelor of Dental Surgery (BDS), College of Dentistry, King Saud University, Riyadh, Saudi Arabia

Professional and Research Experience

2018 Author of the Standard Operating Procedure (SOP no.: L735) for Optical Coherence Tomography (SS-OCT, IVS-300, Santec) Scanning and Analysis Procedures, Oral Health Research Institute, Indiana University

2018 Author of the Standard Operating Procedure (SOP no.: L725) for Micro-Computed Tomography (Micro-CT, Bruker) Scanning and Analysis Procedures, Oral Health Research Institute, Indiana University

2014 Volunteered as a lab instructor for “Technology Based Caries Detection Methods” session in the Orofacial Biology II predoctoral dental course, Indiana University School of Dentistry, at Indiana University-Purdue University, Indianapolis, Indiana, USA

2012-2014	Resident, Operative Dentistry Dental Clinics, Indiana University School of Dentistry, at Indiana University-Purdue University, Indianapolis, Indiana, USA
2011-2012	Teaching Assistant, Department of Operative Dentistry, King Saud bin Abdul Aziz University for Health Sciences, Riyadh, Saudi Arabia
2010-2011	Dental Intern at Riyadh Military Hospital, King Saud University Dental Clinics and King Abdulaziz University Hospital, Riyadh, Saudi Arabia
2009	Leader of the Fifth Year Dental Public Health Project: "A research study of Oral health Education for Primary School Female Students in Riyadh". This project was applied to more than 600 school children and sponsored by Alrajhi Bank and Klynveld Peat Marwick Goerdeler [KPMG] company

Honors, Awards and Grants

2017	Received Certificate of Appreciation for contribution of a member of volunteering team of Academic Guide for Studying at IUPUI, Saudi Students Club, IUPUI, Indianapolis, IN, USA
2017	Received Certificate of Appreciation for supporting Saudi Students Clubs in Indianapolis and Artal Volunteering Efforts activities and programs, Saudi students Club Indianapolis and Saudi Arabian Cultural Mission to the U.S., USA
2016	Received Graduate Professional Educational Grant (G-PEG), IUPUI, Indianapolis, IN, USA

2015 Received Graduate Professional Educational Grant (G-PEG), IUPUI, Indianapolis, IN, USA

2014 Received Dental Master's Thesis Grant Award from Delta Dental Foundation, MI, USA

2011 Received Certificate of Appreciation for contribution at the 15th Kuwait Dental Association International Scientific Conference, Kuwait

2010 Received Certificate of Appreciation for Outstanding Performance during internship training at Riyadh Military Hospital

Peer-Reviewed Publications

2019 Alghilan, M. A., Lippert, F., Platt, J. A., Eckert, G. J., González-Cabezas, C., Fried, D., & Hara, A. T. (2019). Impact of surface micromorphology and demineralization severity on enamel loss measurements by cross-polarization optical coherence tomography. *Journal of dentistry*. 81, 52-58

2017 Alghilan, M. A., Windsor, L. J., Palasuk, J., & Yassen, G. H. (2017). Attachment and proliferation of dental pulp stem cells on dentine treated with different regenerative endodontic protocols. *International Endodontic Journal*. 50(7), 667-675

2015 Alghilan, M. A., Cook, N. B., Platt, J. A., Eckert, G. J., & Hara, A. T. (2015). Susceptibility of restorations and adjacent enamel/dentine to erosion under different salivary flow conditions. *Journal of Dentistry*. 43(12), 1476-1482

2013 Faden A., Abdullah E., Al-Ghilan M., & N. Maflehi. (2013). Oral Cancer: A Clinicopathological Study of 60 Cases. A Single Institution Experience. *Egyptian Dental Journal*. 59(2):1257

Published Abstracts: Presented as Posters or Oral Presentation

2019 Alghilan M. A., Lippert F., Platt J. A., Eckert G. J., González-Cabezas C., Fried D., Hara A. T. (2019, April). CP-OCT Enamel Thickness Measurement on Simulated Erosive Tooth Wear. Poster presented at the Indiana University School of Dentistry Research Day, Indianapolis, IN, USA

2018 Alghilan M. A., Lippert F., Platt J. A., Eckert G. J., González-Cabezas C., Fried D., Hara A. T. (2018, April). Impact of Surface Micromorphology and Demineralization on Enamel Loss Measurements by Cross-Polarization Optical Coherence Tomography. Poster presented at the Indiana University School of Dentistry Research Day, Indianapolis, IN, USA

2017 Alghilan, M. A., Patel, J., Krishnan A., & Thyvalikakath T. P. (2017, April). Extracting Non-Carious Cervical Lesion (NCCL) Conditions from Electronic Dental Records. Poster presented at the Indiana University School of Dentistry Research Day, Indianapolis, IN, USA

2016 Alghilan, M. A., Windsor, L. J., Palasuk, J., & Yassen, G. H. (2016, April). Pulp Stem Cells Attachment and Proliferation After Endodontic Regenerative Protocols. Poster presented at the annual conference of American Association for Dental Research, Los Angeles, Calif, USA and

the Indiana University School of Dentistry Research Day, Indianapolis, IN, USA

2015 Alghilan M. A., Cook N. B., Platt J., Eckert G., Hara A. T. (2015, April). Erosion and Simulated Salivary-Flow Effects on Restorations and Adjacent Tooth. Poster presented at the Indiana University School of Dentistry Research Day, Indianapolis, IN, USA

2015 Alghilan M. A., Cook N. B., Platt J., Eckert G., Hara A. T. (2015, March). Erosion and Simulated Salivary-Flow Effects on Restorations and Adjacent Tooth. Paper presented orally at the annual conference of International Association for Dental Research, Boston, Mass, USA

Conferences, Meetings and Workshops Attended

2019 Indiana University School of Dentistry Research Day, Indianapolis, IN, USA

2018 "Piazza for collaborative learning and problem-solving" webinar, Indiana University, Indianapolis, IN, USA

2018 "Networking for Research" lecture, Indiana University, Indianapolis, IN, USA

2018 "Structuring your research paper" lecture, Indiana University, Indianapolis, IN, USA

2018 Grant Writers' Seminar and Workshop, Indiana University, Indianapolis, IN, USA

2018 "Video conferencing with Zoom: Engaging your students online" webinar, Indiana University, Indianapolis, IN, USA

2018	"Creating a Syllabus" webinar, Indiana University, Indianapolis, IN, USA
2018	"Lecturing with Learner in Mind" webinar, Indiana University, Indianapolis, IN, USA
2018	Indiana University School of Dentistry Research Day, Indianapolis, IN, USA
2017	Indiana University School of Dentistry Research Day, Indianapolis, IN, USA
2016	Indiana University School of Dentistry Research Day, Indianapolis, IN, USA
2016	The annual conference of American Association for Dental Research, Los Angeles, Calif, USA
2015	"Applied molecular biology" workshop, Indiana University, Indianapolis, IN, USA
2015	Indiana University School of Dentistry Research Day, Indianapolis, IN, USA.
2015	The annual conference of International Association for Dental Research, Boston, Mass, USA
2013	"TMD and Occlusion -What Does the Evidence Say?" Maynard K Hine Scholarship Lecture, Indianapolis, IN, USA.
2011	"Basic Medication Safety" lecture, Riyadh Military Hospital, Riyadh, Saudi Arabia

2011	"Anterior Composite, Guidelines for the Success" Hands-on Workshop, Riyadh, Saudi Arabia
2011	Kuwait Dental Association International Scientific Conference & Workshops, Kuwait
2011	"Laminate Veneers" workshop, Riyadh, Saudi Arabia
2010 -2012	Saudi Endodontic Society, Saudi Orthodontic Society and Saudi Dental Society scientific activities
2010	5th Riyadh International Meeting, Riyadh, Saudi Arabia
2010	2nd AGD Day, "Challenge and solutions", Riyadh, Saudi Arabia
2010	Interceptive and Adjunctive Orthodontics CME Activity, Riyadh, Saudi Arabia
2010	Special Care Dentistry Conference, Riyadh, Saudi Arabia
2009	New Dental Era International Conference, Riyadh, Saudi Arabia
2008	Nobel Biocare Dental Implant Workshop, hands on course, King Saud University, Riyadh, Saudi Arabia
2008	The 12th Saudi International Dental Meeting, Riyadh, Saudi Arabia

Membership in Scientific Organizations

International and American Associations for Dental Research

Indiana Section of the American Associations for Dental Research

Saudi Dental Society

American Academy of Cosmetic Dentistry

Saudi Endodontic Society

Saudi Orthodontic Society